Contribution from the Department of Chemistry,
University of British Columbia, Vancouver, British Columbia, Canada V6T 1Z1

Hydrido Thiolato and Thiolato Complexes of Ruthenium(II) Carbonyl Phosphines

Philip G. Jessop, Steven J. Rettig, Chung-Li Lee, and Brian R. James*

Received March 29, 1991

Oxidative addition of RSH (R = H, alkyl, aryl) or RSSR (R = aryl) to $Ru(CO)_2L_3$ (L = PPh_3, **1**) yields respectively *cct*-$RuH(SR)(CO)_2L_2$ (type **2**) (*cct* = *cis,cis,trans*) or *cct*-$Ru(SR)_2(CO)_2L_2$ (type **3**); a hydrido selenolate species is made similarly using PhSeH. Methods for in situ formation of corresponding mixed bis(thiolate) species are also given. **1** is generally unreactive toward thioethers, although with propylene sulfide *cct*-$Ru(\eta^2\text{-}S_2)(CO)_2L_2$ is produced. Metathesis reactions of *cct*-$RuCl_2(CO)_2L_2$ with NaSR salts yield **3** (R = aryl) or, when R = Et, *cct*-$RuCl(SEt)(CO)_2L_2$ or $[L(CO)_2Ru(\mu_2\text{-}SEt)_2(\mu_3\text{-}SEt)Na(THF)]_2$ (**4**), depending on reaction conditions. The complexes are characterized by IR spectroscopy, ^1H, ^{31}P, and, in some cases, ^{13}C NMR spectroscopy, and for **2g** and **3g** (R = SC_6H_4pMe) and **4**, X-ray crystallography. All three complexes crystallized in the space group $P\bar{1}$. For **2g**, a = 12.340 (4) Å, b = 14.948 (3) Å, c = 10.684 (4) Å, α = 90.05 (3)°, β = 99.27 (3)°, γ = 86.84 (3)°, V = 1942 (1) Å^3, and Z = 2; the structure refined to R = 0.032 and R_w = 0.037 for 7174 reflections with $F_o^2 > 3\sigma(F_o^2)$. Corresponding crystallographic data for **3g** are a = 13.173 (3) Å, b = 19.766 (4) Å, c = 9.770 (4) Å, α = 98.26 (2)°, β = 91.24 (3)°, γ = 78.31 (2)°, V = 2465 (1) Å^3, Z = 2, R = 0.041, and R_w = 0.043 for 3597 reflections; for **4**, a = 12.189 (3) Å, b = 13.124 (3) Å, c = 12.032 (4) Å, α = 99.70 (2)°, β = 110.61 (2)°, γ = 67.95 (2)°, V = 1668.4 (8) Å^3, Z = 1, R = 0.039, and R_w = 0.043 for 4252 reflections. **4** has an unprecedented network of transition-metal and alkali-metal ions bridged by thiolate ligands: four thiolates bridge one Ru and one Na, and two thiolates bridge one Ru and two Na atoms. The geometries at Ru and Na are close to octahedral and square pyramidal, respectively. Trends are noted for the ^1H NMR shifts and $^2J_{PH}$ values for the hydride in **2**, and an additivity rule formulated for the ^{31}P shift within the *cct*-$Ru(SR)(SR')(CO)_2(PPh_3)_2$ species. Limited kinetic data suggest that the oxidative addition reactions to **1** probably proceed via a nonradical process, following dissociation of a PPh_3 ligand.

Introduction

The mechanism of the hydrodesulfurization (HDS) of sulfur-containing organics in fuels as operated commercially using heterogeneous Mo-based catalysts[1] remains a mystery, even after decades of research. Even the kinetics of the reaction, outside of the adsorption and desorption steps, are not understood. Analogies to the reactions of homogeneous complexes can lead to greater understanding of such a heterogeneous catalysis and are central to a mechanism proposed recently for thiophene HDS.[2] While such research has emphasized thiophenes because of their resistance to desulfurization, much research into the coordination chemistry of sulfur, thiols, thioethers, disulfides, and other sulfur compounds has identified many modes of coordination of such ligands and the reactivity patterns of their complexes. However, the kinetics of the formation and subsequent reactions of such complexes have been largely ignored. Research was initiated in this laboratory about 5 years ago on the interaction of some Ru(0) complexes and/or their dihydrido derivatives with the S-containing compounds noted above, the use of Ru being dictated partly by the known, high HDS activity of ruthenium sulfides.[1] This present article describes such interactions, especially the full characterization of some (thiolato)ruthenium(II) products and their alternative preparations via metathesis reactions of chlororuthenium(II) complexes. Portions of this work have been reported in two preliminary publications.[3,4]

Experimental Section

All the Ru complexes were synthesized from $RuCl_3 \cdot 3H_2O$, donated by Johnson Matthey Ltd. The various S-containing reagents and PhSeH were Aldrich products; H_2S was a Matheson CP grade product. Diphenyl sulfide was purified by mixing 1:1 with acetone, adding a concentrated acetone solution of $KMnO_4$ until the mixture stayed purple, and filtering and fractionally distilling under vacuum; purity was confirmed by elemental analysis and NMR spectroscopy. Sodium ethane- and *p*-toluenethiolates were synthesized by the reaction of the thiol with an excess of Na in undistilled diethyl ether under N_2; after 1 h, unreacted Na was removed with tweezers and the white suspension of the required salt filtered out, dried under vacuum overnight, and stored under Ar.

Solvents were dried by refluxing for several days over Na and benzophenone (for THF and hexanes) or K_2CO_3 (for acetone) under N_2 and distilling immediately before use. *N,N*-Dimethylacetamide (DMA) for use in the synthesis of $RuH(Cl)(CO)_2(PPh_3)_2$ was instead degassed by repeated freeze/thaw cycles under H_2. Deuterated solvents for NMR use were stored and handled under Ar.

The precursor complexes $Ru(CO)_2(PPh_3)_3$, $Ru(CO)_3(PPh_3)_2$, *cct*-$Ru(H)_2(CO)_2(PPh_3)_2$ (*cct* = *cis,cis,trans*), and *cct*-$RuCl_2(CO)_2(PPh_3)_2$ were prepared by published methods.[5,6] The known complex *cct*-$Ru(H)Cl(CO)_2(PPh_3)_2$[7,8] was prepared by a method which is based on that reported to yield *tcc*-$RuCl_2(CO)_2(PPh_3)_2$ (described below).[7]

Except where noted, synthetic scale reactions were performed in THF at room temperature under 1 atm of N_2 or Ar, using standard Schlenk tube techniques. NMR-scale in situ experiments were performed in the following manner. NMR tubes containing known weights of the solid reagents and the solvent, usually C_6D_6, were sealed under an inert gas with a septum. A liquid reagent or reagent solution was then injected through the septum to start the reaction. NMR spectra were recorded on a Varian XL-300 (for in situ experiments), a Bruker WH-400 (for selective decoupling and COSY experiments), or a Bruker AMX-500 instrument (for the HETCOR experiment). Solid-state ^{13}C NMR spectra were recorded on a Bruker MSL-400 instrument by Dr. L. Randall of this department; the spectrometer contained Zr spinners and a standard MAS probe tuned to 100.6 MHz. The solid-state spectra were obtained with adamantane as an external reference and are reported with respect to TMS. Solution NMR chemical shifts in C_6D_6 were measured with respect to external TMS for ^1H and $^{13}C\{^1H\}$ and external PPh_3 at −6.05 ppm for $^{31}P\{^1H\}$. The shift for PPh_3 with respect to aqueous 85% H_3PO_4, reported previously as −5.9 ppm,[9] was redetermined by acquiring the ^{31}P spectrum in a 10-mm NMR tube fitted with a concentric 5-mm NMR tube containing the H_3PO_4 solution; ^{31}P shifts are reported relative to H_3PO_4, downfield shifts being positive. NMR data listed in this section were all recorded at room temperature (rt).

UV/vis spectra of solutions in quartz cells, closed under argon, were recorded on a Perkin-Elmer 552A spectrometer with a temperature-controlled cell holder (±0.2 °C). Infrared spectra were taken in a Nicolet 5DX FT-IR instrument internally calibrated with a He/Ne laser. FAB-MS spectra of samples in a *p*-nitrobenzyl alcohol matrix were acquired using an AEI MS 9 mass spectrometer with a 6-kV ion source, a 7–8-kV, 1-mA xenon gun, and a 10 s/decade scan rate. The conductivity of solutions was measured with a Yellow Springs Instrument Co.

(1) Chianelli, R. R. *Catal. Rev.* **1984**, *26*, 361.
(2) Angelici, R. *Acc. Chem. Res.* **1988**, *21*, 387.
(3) Lee, C.-L.; Chisholm, J.; James, B. R.; Nelson, D. A.; Lilga, M. A. *Inorg. Chim. Acta* **1986**, *121*, L7.
(4) Jessop, P. G.; Rettig, S. J.; James, B. R. *J. Chem. Soc., Chem. Commun.* **1991**, 773.
(5) Nelson, D. A.; Hallen, R. T.; Lee, C.-L.; James, B. R. In *Recent Developments in Separation Science*; Li, N. N., Calo, J. M., Eds.; CRC Press: Boca Raton, FL, 1986; Vol. IX, pp 1–14.
(6) Porta, F.; Cenini, S.; Giordano, S.; Pizzotti, M. *J. Organomet. Chem.* **1978**, *150*, 261.
(7) James, B. R.; Markham, L. D.; Hui, B. C.; Rempel, G. L. *J. Chem. Soc., Dalton Trans.* **1973**, 2247.
(8) Grundy, K. R. *Inorg. Chim. Acta* **1981**, *53*, L225.
(9) Kosolapoff, G. H.; Maier, L. In *Organic Phosphorus Compounds*, 2nd ed.; Wiley Interscience: New York, 1972; Vol. 1, p 130.

0020-1669/91/1330-4617$02.50/0

Table I. Spectroscopic Data for *cct*-RuH(ER)$(CO)_2(PPh_3)_2$ Complexes[a]

complex[b]	ER	$\delta(^{31}P\{^1H\})$[c]	δ(RuH) ($^2J_{PH}$)[d]	$\delta(^1H)$ (J, assgnt)	ν(RuH)[e]	ν(CO)[e]
2a	SH	42.01	−4.79 (20.1)	−3.00 (dt, $^3J_{PH}$ = 4.9, $^3J_{HH}$ = 2.6, SH)[f]	1901	2029, 1984[g]
2b	SMe	37.14	−4.68 (20.5)	1.04 (s, CH_3)	1899	2021, 1970
2c	SEt	37.25	−4.67 (20.4)	0.77 (t, $^3J_{HH}$ = 7.4, CH_3)	1925	2025, 1964[g]
				1.28 (q, $^3J_{HH}$ = 7.4, CH_2)[h]		
2d	SCH_2Ph	37.09	−4.63 (20.3)	2.53 (s, CH_2)	*i*	2019, 1981
2e	SPh	37.26	−4.32 (19.5)		1920	2030, 1981
2f	SC_6F_5	38.45	−4.31 (19.5)			
2g	SC_6H_4pMe	37.43	−4.33 (19.5)	2.04 (s, CH_3)	1900	2021, 1987[g]
2h	SC_6H_4mMe	37.39	−4.36 (19.5)	1.93 (s, CH_3)	1906	2026, 1983[g]
2i	SC_6H_4oMe	36.55	−4.23 (19.5)	2.19 (s, CH_3)	1900	2025, 1991[g]
2j	SePh	36.98	−4.75 (19.8)		1919	2027, 1978

[a] NMR data in C_6D_6 at 20 °C; δ in ppm; J values in Hz; s = singlet, d = doublet, t = triplet, q = quartet, and m = multiplet. [b] The **a** assignment is specific to an −SH derivative; similarly **b**, **c**, etc. are specific to −SMe, −SEt, etc., as defined here. [c] Singlet. [d] Triplet except for **2a** which is a dt ($^3J_{HH}$ = 3.1). [e] IR, cm^{-1} in Nujol. [f] Also δ 7.98 (m, 12 H, *o*-H), 7.03 (m, 18 H, *p*-, *m*-H). [g] In CH_2Cl_2: **2a** (2035, 1979), **2c** (2029, 1971), **2g** (2033, 1975), **2h** (2035, 1975), and **2i** (2035, 1977). [h] Also δ 7.95 (m, 12 H, *o*-H), 6.29 (m, 18 H, *p*-, *m*-H). $^{13}C\{^1H\}$ NMR: δ 19.86 (s, CH_3), 28.06 (s, CH_2), 128.21 (t, $|J_{CP} + J_{CP'}|$ = 4.4 Hz, *m*-C), 130.07 (s, *p*-C), 134.55 (t, $|J_{CP} + J_{CP'}|$ = 5.9, *o*-C), 135.6 (t, $|J_{CP} + J_{CP'}|$ = 23.3 Hz, P–C). [i] ν(RuH) not detected.

Table II. Spectroscopic Data for *cct*-Ru(SR)(SR′)$(CO)_2(PPh_3)_2$ Complexes[a]

complex[b]	R	R′	$\delta(^{31}P\{^1H\})$:found (calcd)[c]	$\delta(^1H)$ of thiolate ligand (J, assgnt)
3a[d,e]	H	H	20.40 (21.47)	−1.93 (t, $^3J_{PH}$ = 6.8, SH)[f]
3ag[g]	H	C_6H_4pMe	16.62 (16.17)	−1.82 (t, $^3J_{PH}$ = 7.1, SH)
3ae[g]	H	Ph	16.56 (16.07)	−1.82 (t, $^3J_{PH}$ = 7.3, SH)
3f[g]	C_6F_5	C_6F_5	18.30 (18.25)	
3ef[g]	Ph	C_6F_5	14.42 (14.46)	
3c[e]	Et	Et	11.18 (11.21)	1.16 (t, $^3J_{HH}$ = 7.4, CH_3)
				1.97 (q, $^3J_{HH}$ = 7.4, CH_2)[h]
3cg[g]	Et	C_6H_4pMe	11.00 (11.04)	
3g[e]	C_6H_4pMe	C_6H_4pMe	10.90 (10.87)	2.03 (s, CH_3)
				6.54 (d, $^3J_{HH}$ = 8.1, *o*-H)
				6.86 (d, $^3J_{HH}$ = 8.2, *m*-H)[i]
3eg[g]	Ph	C_6H_4pMe	10.78 (10.77)	
3e[g]	Ph	Ph	10.69 (10.67)	
3h[j]	C_6H_4mMe	C_6H_4mMe	11.77	

[a] As for Table I. [b] As for Table I; e.g. **3c** refers to R and R′ = Et, while **3ag** refers to R = H and R′ = C_6H_4pMe. [c] Singlet; calculated from the empirical equation given in the text. [d] Details on the synthesis of **3a**, described briefly in a communication,[3] will be published later together with crystallographic and H/D exchange data.[11] [e] IR, ν(CO), cm^{-1}, in Nujol: **3a** (2046, 1981), **3c** (2022, 1963), **3g** (2028, 1968). [f] Also, δ 8.18 (m, 12 H, *o*-H), 6.98 (m, 18 H, *m*-, *p*-H). [g] Species formed in situ in C_6D_6. [h] Also, δ 8.22 (m, 12 H, *o*-H), 7.04 (m, 18 H, *m*-, *p*-H). [i] The *o*- and *m*-H assignments may be reversed. Also, for PPh_3 ligands, δ 7.95 (m, 12 H, *o*-H), 6.99 (m, 18 H, *m*-, *p*-H). [j] Species formed in situ in CD_2Cl_2; $^{31}P\{^1H\}$ singlets in CD_2Cl_2 for **3a** and **3e** at 21.90 and 11.43 ppm, respectively.

Model 3403 cell (with a cell constant of 1 cm^{-1}) and a Serfass Model 15B1 conductivity bridge. Microanalyses were performed by Mr. P. Borda of this department.

Reaction of $Ru(CO)_2(PPh_3)_3$ (1) with H_2S, Thiols, and a Selenol. $Ru(CO)_2(PPh_3)_3$ (400 mg, 0.4 mmol) in THF (50 mL) was reacted with (a) gaseous H_2S at 1 atm and −35 °C for 2 h,[3] (b) gaseous MeSH at 1 atm at room temperature for 3 h, (c) excess (e.g. 8 equiv) thiol at room temperature for 3 h, and (d) 1 equiv of benzeneselenol for 1.5 h at room temperature. The solvent volume was then reduced to ~5 mL by vacuum distillation, and hexanes (100 mL) was added to induce precipitation of the product (40–95% yields). This was isolated by filtration to give in (a) a pale tan powder and in (b–d) a yellow powder, which generally analyze correctly for RuH(ER)$(CO)_2(PPh_3)_2$ (Table S-I, supplementary material). In the H_2S and MeSH reactions, these gaseous reagents at 1 atm are present in large excess; such a condition is not essential for the syntheses and results merely from the convenient use of 1 atm.

The carbon analyses of **2e** and **2g** are 1% low, while complex **2f** was isolated but not purified; from the spectroscopic data (Table I) there is no doubt about the identity of **2e–g**. The same series of products (**2**) can be prepared similarly using *cct*-$RuH_2(CO)_2(PPh_3)_2$ as the precursor in reactions which liberate H_2.[3]

Complex **1** shows no reaction with ethanol under conditions used for the thiol reactions.

Reaction of $Ru(CO)_2(PPh_3)_3$ (1) with Disulfides. Complex **1** (140 mg, 0.15 mmol) and *p*-tolyl disulfide (91 mg, 0.36 mmol) were dissolved in THF (20 mL) in a Schlenk tube wrapped with foil in a darkened room. The solution remained orange throughout the reaction. After 4.5 h, the volume of the solution was reduced to 5 mL by vacuum distillation, and hexanes (60 mL) was added to induce precipitation. The collected yellow solid was *cct*-$Ru(SC_6H_4p\text{Me})_2(CO)_2(PPh_3)_2$ (**3g**, 85% yield): UV/vis, λ_{max} (in THF) 430 nm (ϵ 3000 M^{-1} cm^{-1}); IR (Nujol) 2028, 1968 cm^{-1} (ν(CO)); ^1H NMR (C_6D_6) δ 2.03 (s, 6 H, CH_3), 6.54 (d, 4 H, $^3J_{HH}$ = 8.1 Hz, SC_6H_4), 6.86 (d, 4 H, $^3J_{HH}$ = 8.2 Hz, SC_6H_4), 6.99 (m, 18 H, *p*-, *m*-PPh_3), 7.95 (m, 12 H, *o*-PPh_3); $^{13}C\{^1H\}$ NMR (C_6D_6) δ 20.90 (s, CH_3); $^{31}P\{^1H\}$ NMR (C_6D_6) δ 10.95 (s).

The reaction was monitored also by $^{31}P\{^1H\}$ NMR spectroscopy in an NMR tube at 18 °C under Ar (4.2 mg of **1** and 31.7 mg of disulfide in 0.5 mL of C_6D_6). The pseudo-first-order log plot for loss of **1** was linear for at least 3 half-lives, with a measured rate constant of 1.2×10^{-3} s^{-1}, which was essentially unchanged when the reaction was carried out in the presence of a large excess (0.13 mL) of 1,1-dicyclopropylethylene, a thiyl radical trap.[10] In the presence of added, excess PPh_3 (phosphine:Ru ≈ 30), **2g** (the hydrido thiolato derivative) and $OPPh_3$ were formed as well as **3g**. The species *cct*-$Ru(SR)_2(CO)_2(PPh_3)_2$, where R = Ph (**3e**) or C_6F_5 (**3f**) (Table II), were formed in situ by reaction of *cct*-$Ru(H)_2(CO)_2(PPh_3)_2$ with the RSH thiol (see below). Reactions of **1** with alkyl sulfides were more complex than with aryl disulfides; e.g., reaction of **1** (3.3 mg) with ethyl disulfide (35 μL) in 0.5 mL of C_6D_6 at 18 °C showed, after 2 h, low conversion to a mixture of the hydrido thiolato species **2c** (6%) and *cct*-$Ru(SEt)_2(CO)_2(PPh_3)_2$ (**3c**, 12%) (see below).

Reaction of *cct*-$Ru(H)_2(CO)_2(PPh_3)_2$ with Mixtures of Thiols. The dihydrido precursor (4.6 mg, 6.9 μmol) and *p*-thiocresol (24 mg, 0.20 mmol) were dissolved in C_6D_6 (~1 mL) under argon in an NMR tube capped with a septum. Thiophenol (20 μL, 0.20 mmol) was injected through the septum, and after 7 h at 21 °C, the products were *cct*-RuH(SPh)$(CO)_2(PPh_3)_2$ (**2e**, 46%), *cct*-RuH$(SC_6H_4p\text{Me})(CO)_2(PPh_3)_2$ (**2g**, 21%), *cct*-$Ru(SPh)_2(CO)_2(PPh_3)_2$ (**3e**, 12%), *cct*-Ru(SPh)-$(SC_6H_4p\text{Me})(CO)_2(PPh_3)_2$ (**3eg**, 15%), and *cct*-$Ru(SC_6H_4p\text{Me})_2$-$(CO)_2(PPh_3)_2$ (**3g**, 6%). Experiments with other mixtures of thiols were performed in a similar manner. The mixed species (e.g. **3eg**) could be formed in situ via treatment of bis(thiolato) species with a second thiol

(10) Campredon, M.; Kanabus-Kaminska, J. M.; Griller, D. *J. Org. Chem.* **1988**, *53*, 5393.

(e.g. from **3g** with PhSH); the mixed-thiolato species are similarly formed from **3a**[3,11] with RSH. The NMR data of the mixed thiolates are given in Table II.

Reaction of $Ru(CO)_2(PPh_3)_3$ (1) with Thioethers. A solution of propylene sulfide (2 mL, 30 mmol) and **1** (0.4 g, 0.5 mmol) in THF (50 mL) was stirred overnight at 18 °C. The precipitated solid (70% yield) was collected and shown to be *cct*-$Ru(\eta^2\text{-}S_2)(CO)_2(PPh_3)_2$ by elemental analysis (C, H, S; Table S-I, supplementary material) and spectroscopy: IR (Nujol) 2010, 1950 cm^{-1} (ν(CO)); ^1H NMR (C_6D_6) δ 6.99 (m, 12 H, *m*-H), 7.16 (s, 6 H, *p*-H), 7.77 (m, 12 H, *o*-H); $^{31}P\{^1H\}$ NMR (CD_2Cl_2) δ 39.53 (s) (a trace signal at δ 42.10 results from the presence of $SPPh_3$).

Complex **1** was unreactive toward dialkyl, diaryl, and alkyl aryl sulfides and thiophene under corresponding conditions.

Reaction of $Ru(CO)_3(PPh_3)_2$ with H_2S. A refluxing THF (40 mL) solution of $Ru(CO)_3(PPh_3)_2$ (600 mg, 0.85 mmol), after being under H_2S (1 atm) for 3 h, was evaporated to dryness; the residue showed 5% conversion to each of *cct*-$RuH(SH)(CO)_2(PPh_3)_2$ (**2a**) and *cct*-$Ru(SH)_2(CO)_2(PPh_3)_2$ (**3a**), as determined by ^{31}P NMR spectroscopy (Table II), the remainder being unreacted starting material.

Reaction of *cct*-$RuCl_2(CO)_2(PPh_3)_2$ with $NaSC_6H_4p$Me. An acetone (40 mL) suspension of the white dichloride (140 mg, 0.18 mmol) and the thiolate salt (56 mg, 0.38 mmol) under 1 atm of CO turned yellow within 1 min at 20 °C. The NaCl was filtered off and the yellow filtrate reduced in volume to 10 mL by evacuation; addition of MeOH (10 mL) precipitated the pure dithiolato complex **3g**.

Reaction of *cct*-$RuCl_2(CO)_2(PPh_3)_2$ with NaSEt. (a) An acetone (20 mL) white suspension of the dichloride (450 mg, 0.60 mmol) and the thiolate (120 mg, 1.4 mmol) under 1 atm of CO turned yellow within 1 min at 20 °C. The suspension was stirred overnight and then filtered through diatomaceous earth. The volume of the yellow filtrate was reduced to 5 mL by evacuation, MeOH (30 mL) was added, and the vessel was left for 2 h at 0 °C. The resulting yellow precipitate was filtered out and collected; the product was a mixture of *cct*-$Ru(SEt)_2(CO)_2(PPh_3)_2$ (**3c**) (Table II) and PPh_3. Attempts at purifying this complex or repeating the reaction resulted in yellow or brown oils which also contained **3c**.

(b) A THF (180 mL) yellow suspension of the dichloride (520 mg, 0.70 mmol) and the thiolate (1.4 g, 17 mmol) was stirred under Ar for 1 h at room temperature and then filtered; the filtrate was evaporated to dryness and the residue redissolved in THF (10 mL) and reprecipitated by addition of hexane (100 mL). Elemental analysis (Table S-I, supplementary material), spectroscopic data, and an X-ray analysis (see below) showed the product to be $[(PPh_3)(CO)_2Ru(\mu\text{-}SEt)_3Na(THF)]_2$ (**4**, 53% yield): IR (Nujol) 2014, 1952 cm^{-1} (ν(CO)); ^1H NMR (C_6D_6) δ 1.41 (t, 12 H, $^3J_{HH}$ = 7.6 Hz, $CH_3(a)$), 1.41 (m, 8 H, β-CH_2 of THF), 1.59 (t, 6 H, $^3J_{HH}$ = 7.3 Hz, $CH_3(b)$), 2.71 (dq, 8 H, $^2J_{HH}$ = 9.0, $^3J_{HH}$ = 7.3 Hz, $CH_2(a)$), 2.95 (dq, 8 H, $^2J_{HH}$ = 9.0, $^3J_{HH}$ = 7.5 Hz, $CH_2(a)$), 2.97 (dq, 4 H, $^2J_{HH}$ = 9.0, $^3J_{HH}$ = 7.3 Hz, $CH_2(b)$), 2.98 (dq, 4 H, $^2J_{HH}$ = 9.0, $^3J_{HH}$ = 7.5 Hz, $CH_2(b)$), 3.57 (m, 8 H, α-CH_2 of THF), 7.06 (m, 6 H, *p*-H), 7.15 (t, 12 H, $^3J_{HH}$ = 7.0 Hz, *m*-H), 7.96 (t, 12 H, $^3J_{HH}$ = 8.8 Hz, *o*-H); $^{13}C\{^1H\}$ NMR (C_6D_6, 75 MHz) δ 20.73 ($CH_3(b)$), 20.89 ($CH_3(a)$), 25.16 ($CH_2(a)$), 25.71 (β-C of THF), 26.62 ($CH_2(b)$), 67.85 (α-C of THF), 128.16 (*p*-C), 130.22 (*m*-C), 134.50 (d, J_{PC} = 9.4 Hz, *o*-C), 135.28 (d, J_{PC} = 41.9 Hz, P-C), 197.48 (CO); $^{31}P\{^1H\}$ NMR (C_6D_6, 121 MHz) δ 25.05 (s); FAB/MS *m/z* 1326 [(M − THF)$^+$], 1269 [(M − 2CO − THF)$^+$], 1147 [(M − 2SEt − 2CO − THF)$^+$]. A THF solution of **4** (up to 1 mM) under Ar had no detectable conductance at room temperature.

(c) When only 2–3 equiv of NaSEt was used in THF, method b, partial conversion to *cct*-$RuCl(SEt)(CO)_2(PPh_3)_2$ (**5**), is observed. In a synthesis using excess NaSEt (~20 equiv) but reduced reaction times (10–15 min), procedure b yielded **5** (~50% yield) containing trace amounts of **3c**. The analysis for **5** is 1.1% low in C, but the spectroscopic data confirm the formulation: ^1H NMR (C_6D_6, 300 MHz) δ 1.13 (t, 3 H, $^3J_{HH}$ = 7.4 Hz, CH_3), 1.92 (q, 2 H, $^3J_{HH}$ = 7.3 Hz, CH_2), 7.0 (m, 18 H, *m*-, *p*-H), 8.25 (m, 12 H, *o*-H); $^{31}P\{^1H\}$ NMR (C_6D_6) δ 14.54 (s); IR (Nujol) 2042, 1988 cm^{-1} (ν(CO)); FAB/MS *m/z* 778 [(M)$^+$], 750 [(M − CO)$^+$], 722 [(M − 2CO)$^+$], 689 [(M − CO − SEt)$^+$].

Reaction of $RuCl_3\cdot 3H_2O$ with PPh_3 and NaSEt. A brown suspension of the Ru salt (300 mg, 0.96 mmol) and PPh_3 (1.43 g, 5.4 mmol) in refluxing MeOH (30 mL) under N_2 for 15 min turned dark green. The mixture was cooled to 20 °C, NaSEt (155 mg, 1.8 mmol) added, and CO introduced at 1 atm. A brown color returned immediately but again slowly changed to dark green. After 30 min, the volatiles were removed by vacuum distillation, leaving a yellow-brown residue containing (by $^{31}P\{^1H\}$ NMR spectroscopy in C_6D_6) PPh_3, *cct*-$RuCl_2(CO)_2(PPh_3)_2$ (20% of ^{31}P NMR signal excluding that of free PPh_3), *cct*-$RuCl(SEt)(CO)_2(PPh_3)_2$ (**5**, 7%), *cct*-$Ru(SEt)_2(CO)_2(PPh_3)_2$ (**3c**, 19%), a product having the same chemical shift as $[(PPh_3)(CO)_2Ru(\mu\text{-}SEt)_3Na(THF)]_2$ (**4**, 16%), and several unknowns at lower concentrations.

Synthesis of *cct*-$RuH(Cl)(CO)_2(PPh_3)_2$ (6) and Its Reaction with $NaSC_6H_4p$Me. $RuCl_2(PPh_3)_3$ (0.40 g, 0.42 mmol) was dissolved in 10 mL of degassed DMA under 1 atm of H_2, giving a red-brown solution. After 30 min, the H_2 was replaced with 1 atm of CO; the solution subsequently turned yellow within 5 min. After another 30 min, the volume was reduced by vacuum and MeOH (20 mL) added. The resulting white precipitate was filtered out and dried under vacuum (40% yield). The spectroscopic data (^1H, $^{31}P\{^1H\}$, and $^{13}C\{^1H\}$ NMR and IR spectroscopy) matched those reported for **6**.[12]

A white suspension of **6** (72 mg, 0.10 mmol) and $NaSC_6H_4p$Me (18 mg, 0.12 mmol) in acetone (20 mL) at 20 °C under Ar turned yellow within minutes. After 2 h, the volatiles were removed by vacuum distillation leaving a yellow powder containing (by ^1H and $^{31}P\{^1H\}$ NMR spectroscopy in C_6D_6) unreacted **6** (25% of ^{31}P signal), **2g** (55%), **3g** (10%), and small amounts (<5%) of PPh_3, **1**, and $Ru(CO)_3(PPh_3)_2$. An overnight reaction of **6** with 3 equiv of the thiolate produced a mixture of **3g** (90%) and **2g** (10%).

X-ray Crystallographic Analyses of *cct*-$RuH(SC_6H_4p$Me$)(CO)_2(PPh_3)_2$ (2g), *cct*-$Ru(SC_6H_4p$Me$)_2(CO)_2(PPh_3)_2\cdot$THF (3g·THF), and $[(PPh_3)(CO)_2Ru(SEt)_3Na(THF)]_2$ (4). Yellow crystals of the complexes suitable for X-ray crystallography were prepared by diffusion of hexanes into concentrated THF solutions of each complex under Ar in darkness. The crystal data are summarized in Table III. The final unit cell parameters were obtained by least squares on the setting angles for 25 reflections with 2θ = 31.1–35.6° (**2g**), 10.0–16.0° (**3g**), and 20.0–26.5° (**4**). The intensities of three standard reflections, measured every 200 reflections throughout the data collection, were essentially constant (**2g** and **3g**) or decayed uniformly by 12% (**4**). The data were processed[13] and corrected for Lorentz and polarization effects, decay (for **4**), and adsorption (empirical, based on azimuthal scans for four reflections).

The structure analyses were initiated in the centrosymmetric space group $P\bar{1}$, the choices being confirmed by the subsequent successful solutions and refinements of the structures. The structures were solved by conventional heavy-atom methods, the coordinates of the Ru, P, and S atoms being determined from the Patterson functions and those of the remaining non-hydrogen atoms from subsequent difference Fourier syntheses. The asymmetric unit of **3g** contains one THF solvate molecule in addition to the complex molecule. Complex **4** has crystallographically imposed inversion symmetry. All non-hydrogen atoms were refined with anisotropic thermal parameters. Hydrogen atoms were fixed in idealized positions (d_{C-H} = 0.98 Å; B(H) = 1.2 B(bonded atom)), except for the metal hydride in **2g** which was refined with an isotropic thermal parameter. Neutral-atom scattering factors and anomalous dispersion corrections for the non-hydrogen atoms were taken from ref 14. Final atomic coordinates and equivalent isotropic thermal parameters [$B_{eq} = {}^4/_3\sum_i\sum_j b_{ij}(\mathbf{a}_i\cdot\mathbf{a}_j)$], bond lengths, and bond angles appear in Tables IV–VI.

Results and Discussion

Reactions of $Ru(CO)_2(PPh_3)_3$ (1) with Thiols and a Selenol. Complex **1** readily undergoes oxidative addition reactions with H_2S, a range of alkane- and arenethiols, and benzeneselenol (the only selenol tested), according to eq 1 (E = S, Se; R = H, alkyl, aryl). The products **2a–j** of cis,cis,trans (cct) geometry are listed

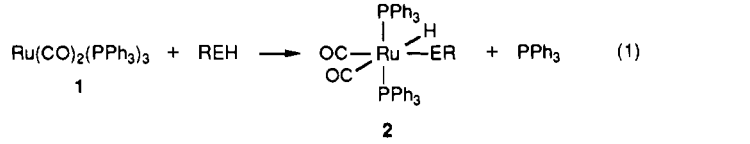

in Table I. The ^1H NMR spectra contain a high-field triplet due to the hydride ligand, split by two equivalent phosphines, the $^2J_{PH}$ values being consistent with phosphines cis to the hydride.[15] The

(11) Lee, C.-L.; Jessop, P. G.; James, B. R.; Lock, C. J. L.; Faggiani, R. To be published.

(12) (a) Dekleva, T. W. Ph.D. Dissertation, University of British Columbia, Vancouver, BC, Canada, 1983. (b) Joshi, A. J.; James, B. R. *Organometallics* **1990**, *9*, 199.

(13) TEXSAN/TEXRAY structural analysis package, which includes versions of the following: DIRDIF, direct methods for difference structures, by P. T. Beurskens; ORFLS, full-matrix least squares, and ORFFE, function and errors, by W. R. Busing, K. O. Martin, and H. A. Levy; ORTEP II, illustrations, by C. K. Johnson.

(14) *International Tables for X-ray Crystallography*; Kynoch Press: Birmingham, U.K., (present distributor Kluwer Academic Publishers, Dordrecht, The Netherlands), 1974; Vol. IV, pp 99–102 and 149.

Table III. Crystallographic Data[a]

compd	**2g**	**3g**·THF	**4**
formula	$C_{45}H_{38}O_2P_2RuS$	$C_{56}H_{52}O_3P_2RuS_2$	$C_{60}H_{76}Na_2O_6P_2Ru_2S_6$
fw	804.86	928.06	1395.68
color, habit	yellow, irregular	yellow, prism	yellow, prism
cryst size, mm	0.30 × 0.35 × 0.50	0.15 × 0.22 × 0.46	0.10 × 0.15 × 0.35
cryst system	triclinic	triclinic	triclinic
space group	$P\bar{1}$	$P\bar{1}$	$P\bar{1}$
a, Å	12.340 (4)	13.173 (3)	12.189 (3)
b, Å	14.948 (3)	19.766 (4)	13.124 (3)
c, Å	10.684 (4)	9.770 (4)	12.032 (4)
α, deg	90.05 (3)	98.26 (2)	99.70 (2)
β, deg	99.27 (3)	91.24 (3)	110.61 (2)
γ, deg	86.84 (3)	78.31 (2)	67.95 (2)
V, Å^3	1942 (1)	2465 (1)	1668.4 (8)
Z	2	2	1
ρ_{calc}, g/cm^3	1.38	1.25	1.39
$F(000)$	826	956	720
μ(Mo Kα), cm^{-1}	5.63	4.91	7.27
transm factors	0.947–1.00	0.926–1.00	0.946–1.00
scan type	ω–2θ	ω–2θ	ω–2θ
scan range, deg in ω	1.31 + 0.35 tan θ	1.16 + 0.35 tan θ	1.26 + 0.35 tan θ
scan speed, deg/min	32	32	16
data collcd	$+h,\pm k,\pm l$	$+h,\pm k,\pm l$	$+h,\pm k,\pm l$
$2\theta_{max}$, deg	60	50	55
cryst decay, %	negligible	negligible	12.0
tot. no. of reflcns	11 794	9129	7986
no. of unique reflcns	11 310	8713	7627
R_{merge}	0.022	0.074	0.040
no. of reflcns with $I > 3\sigma(I)$	7174	3597	4252
no. of variables	464	577	352
R	0.032	0.041	0.039
R_w	0.037	0.043	0.043
gof	1.28	1.17	1.43
max Δ/σ (final cycle)	0.14	0.06	0.02
resid density, e/Å^3	0.55	0.54	0.84 (near Ru)

[a] Temperature 294 K, Rigaku AFC6S diffractometer, Mo Kα radiation (λ = 0.71069 Å), graphite monochromator, takeoff angle 6.0°, aperture 6.0 × 6.0 mm at a distance of 285 mm from the crystal, stationary background counts at each end of the scan (scan:background time ratio 2:1), $\sigma^2(F^2) = [S^2(C + 4B) + (pF^2)^2]/Lp^2$ (S = scan rate, C = scan count, B = normalized background count, p = 0.035 for **2g**, 0.040 for **3g**, and 0.030 for **4**), function minimized $\sum w(|F_o| - |F_c|)^2$, where $w = 4F_o^2/\sigma^2(F_o^2)$, $R = \sum||F_o| - |F_c||/\sum|F_o|$, $R_w = (\sum w(|F_o| - |F_c|)^2/\sum w|F_o|^2)^{1/2}$, and gof = $[\sum(|F_o| - |F_c|)^2/(m - n)]^{1/2}$. Values given for R, R_w, and gof are based on those reflections with $I \geq 3\sigma(I)$.

sharp singlet in the $^{31}P\{^1H\}$ NMR spectra demonstrates equivalent phosphines, their relative positions (trans or cis) being determined by ^1H and $^{13}C\{^1H\}$ NMR data: the differences between the *o*- and *m*-, *p*-H signals of the PPh_3 ligands of the **2** complexes are >0.5 ppm, while the ^{13}C spectrum of **2c** shows triplets for the phenyl carbons. Both these observations are consistent only with trans phosphines.[16] The two ν(CO) bands in the IR spectra indicate cis carbonyls, and the cct geometry is shown generally in eq 1.

Such a structure is confirmed for the *p*-toluenethiolate complex **2g** by a crystallographic analysis (Figure 1; Tables IV–VI). No other monomeric hydrido(thiolato)ruthenium complex has been crystallographically characterized. Deviations from octahedral geometry at the metal result from a crowding of the hydride ligand by the four ligands cis to it; the P–Ru–P and C(1)–Ru–S angles are 172.6 and 167.2°, respectively.

The Ru–S bond length (2.458 Å) is similar to that for the thiolate ligand (2.453 Å) trans to a carbonyl in the complex $Ru(pyS)_2(CO)_2(PPh_3)$ (pyS = *o*-SC_5H_4N).[17] Shorter Ru^{II}–S bonds (2.406–2.429 Å) exist in thiolate ligands trans to weaker π acceptors than CO, such as phosphine or thiolate groups,[17,18] although in $(PhMe_2P)_3Ru(\mu\text{-}SH)_3Ru(PMe_2Ph)_2(SH)$ the terminal

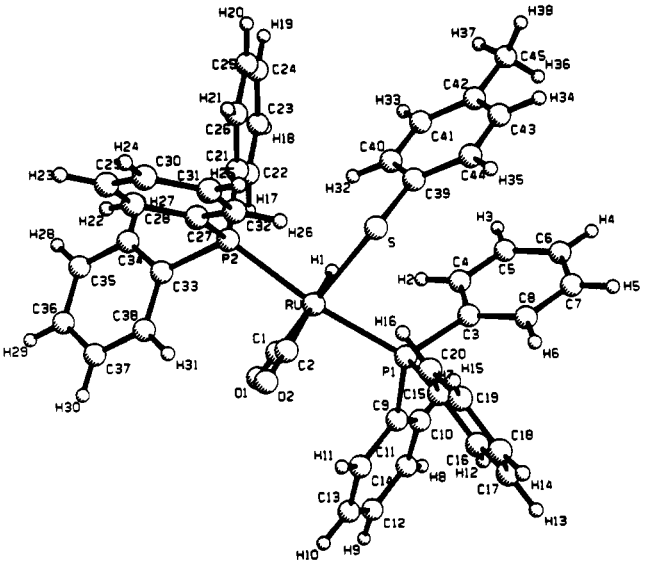

Figure 1. Structure of *cct*-$RuH(SC_6H_4pMe)(CO)_2(PPh_3)_2$ (**2g**).

Ru–S bond length (trans to a bridging SH ligand) is 2.44 Å.[19] The M^{II}–S–C bond angle is relatively large (113.6°) in **2g** as in other complexes with arenethiolates trans to carbonyls, such as in *cis,cis,cis*-$Fe(SPh)_2(CO)_2(Ph_2P(CH_2)_2PPh_2)$ (112.4–114.9°).[20] Smaller angles (107.7–109.6°) are found in complexes with ar-

(15) Hallman, P. S.; McGarvey, B. R.; Wilkinson, G. *J. Chem. Soc. A* **1968**, 3143. Chaudret, B.; Commenges, G.; Poilblanc, R. *J. Chem. Soc., Dalton Trans.* **1984**, 1635. L'Eplattenier, F.; Calderazzo, F. *Inorg. Chem.* **1968**, *7*, 1290.
(16) (a) Mann, B. E.; Shaw, B. L.; Stainbank, R. E. *J. Chem. Soc., Chem. Commun.* **1972**, 151. (b) Moore, D. S.; Robinson, S. D. *Inorg. Chim. Acta* **1981**, *53*, L171.
(17) (a) Mura, P.; Olby, B. G.; Robinson, S. D. *Inorg. Chim. Acta* **1985**, *98*, L21. (b) Mura, P.; Olby, B. G.; Robinson, S. D. *J. Chem. Soc., Dalton Trans.* **1985**, 2101.
(18) Jeannin, S.; Jeannin, Y.; Lavigne, G. *Transition Met. Chem.* **1976**, *1*, 192.
(19) Osakada, K.; Yamamoto, T.; Yamamoto, A.; Takenaka, A.; Sasada, Y. *Inorg. Chim. Acta* **1985**, *105*, L9.
(20) Takacs, J.; Marko, L.; Parkanyi, L. *J. Organomet. Chem.* **1989**, *361*, 109.

enethiolates trans to phosphine or thiolate ligands.[17,18,20] The length (1.875 Å) of the Ru–C bond trans to the thiolate ligand in **2g** is slightly shorter than that found in $Ru(pyS)_2(CO)_2(PPh_3)$ (1.895 Å),[17b] possibly because of the intramolecular interactions which exist in the pyridyl complex. The Ru–C bond trans to hydride is 1.945 Å in **2g** (cf. 1.970 Å in *cct*-$[RuH(H_2O)(CO)_2(PPh_3)_2]^+$),[21] longer than that trans to the thiolate because of the strong trans influence of the hydride ligand.[22] The aquo complex shows inequivalent Ru–P bond lengths that result from crystal packing effects. The Ru–P bond lengths in **2g** are essentially equivalent and match closely those in related complexes.[21,23] The Ru–H bond length in **2g** (1.58 Å) is slightly shorter than those found in $[RuH(H_2O)(CO)_2(PPh_3)_2]^+$ (1.7 Å),[19] $RuH(Cl)(PPh_3)_3$ (1.7 Å),[24] and *trans*-RuH(Cl)(diop)$_2$ (1.65 Å).[25] Other platinum metal complexes related closely to **2** include *cct*-IrH(ER)Cl-$(CO)(PPh_3)_2$ (E = S, Se; R = H, *n*-Pr, *n*-Bu, aryl)[26–28] and $OsH(\eta^1\text{-}Se_2Me)(CO)_2(PPh_3)_2$.[29]

Within the complexes **2a–j**, the chemical shift of the hydride ligand (Table I) moves toward higher fields in the order

$$ER = SC_6H_4oMe < S(aryl) \ll S(alkyl) < SePh < SH$$

The order is consistent with an electronic effect and is approximately paralleled by the order of the shifts (δ_H) for the acidic protons of the REH reagents in the same solvent, C_6D_6:

(aryl)SH	<	MeC_6H_4oSH	≪	(alkyl)SH	~	PhSeH	<	H_2S
3.1 ± 0.1		2.92		1.2 ± 0.2		1.19		0.20

The $^2J_{PH}$ coupling constant (Table I) shows less variation, but the values of 19.5 (S(aryl)), 19.8 (SePh), 20.1 (SH), and 20.4 ± 0.1 Hz (S(alkyl)), together with the δ(Ru–H) value, provide a reliable indication of the nature of the ER group in RuH-$(ER)(CO)_2(PPh_3)_2$ complexes. The $^{31}P\{^1H\}$ NMR singlet shifts to higher field in the order

$$ER = SH \ll SC_6F_5 < S(aryl) < S(alkyl) < SePh < SC_6H_4oMe$$

essentially the reverse of that given above. The ^{31}P shifts appear to depend inversely (and reasonably) on the Ru–P bond lengths, which are likely affected by the bulk of the thiolate-type ligands; the Ru–P bond lengths and shifts of **2g**, **3a**,[11] **3g**, and **4** (the last two being described below) fit remarkably well a correlation noted for a series of ruthenium(II) triphenylphosphine complexes (Figure 2).[12a]

There are no clear trends in IR data for ν(RuH) or ν(CO) (Table I); the asymmetric ν(CO) band varies over 27 cm^{-1} (Nujol), and the higher frequencies noted generally for the arenethiolato ligands may result from the π-acceptor ability of the aromatic ring reducing the π back-bonding from Ru to the CO. Of note, ν(RuH) is not detected in CH_2Cl_2, and this does not result from conversion of the hydride ligand to chloride.

The UV/vis spectra of the **2** complexes in THF show an absorbance maximum near 400 nm, which is probably due to S/Se-to-Ru charge transfer:[30]

	ER					
	SePh	SC_6H_4pMe	SPh	SCH_2Ph	SMe	SEt
λ_{max}, nm	411	398	397	393	395	396
ϵ, M^{-1} cm^{-1}	1900	1900	1900	1300	1100	1000

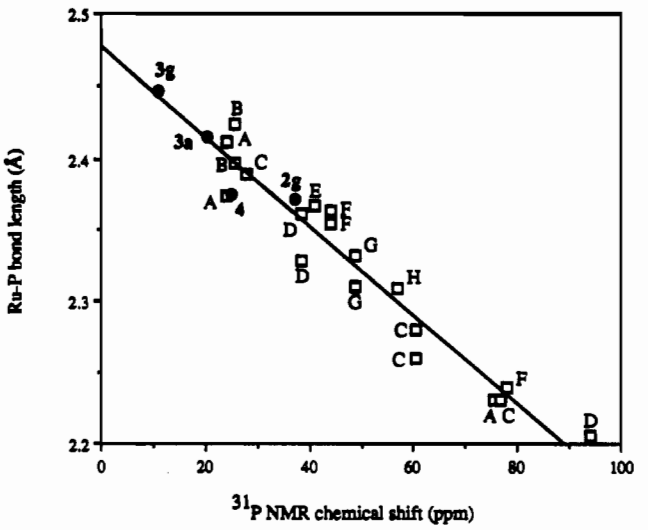

Figure 2. Correlation between solution $^{31}P\{^1H\}$ NMR shifts and Ru–P bond lengths for a series of Ru(II) complexes containing PPh_3 or P-$(C_6H_4pMe)_3$. Key (data reference in parentheses): **2g**, **3g**, and **4** (this work); **3a** (ref 11); A, $RuCl_2(PPh_3)_3$ (ref 58); B, *cct*-$Ru(O_2CPh)_2(CO)_2(PPh_3)_2$ (ref 39); C, $[H_2RuCl\{P(C_6H_4pMe)_3\}_2]_2$ (ref 59); D, RuH-$(Cl)(PPh_3)_3$ (ref 24); E, $Ru(pyS)_2(CO)_2(PPh_3)$ (ref 17); F, RuH-$(O_2CMe)(PPh_3)_3$ (ref 60); G, $[RuH(\eta^6\text{-}C_6H_5PPh_2)(PPh_3)_2]^+$ (ref 61); H, $Ru(pyS)_2(CO)(PPh_3)$ (ref 17). ^{31}P shifts were measured in C_6D_6, except for ref 17 ($CDCl_3$). Three entries for A correspond to the three phosphines, etc.

Such small, unpredictable changes on charge-transfer bands within thiolato complexes have been noted for a series of Mo and Tc species.[31]

Qualitative kinetic data on reaction 1 with H_2S and EtSH at room temperature in THF reveal in each case half-lives of a few seconds, which would appear to be consistent with a mechanism involving a rate-limiting dissociation of PPh_3 from **1**, followed by a faster oxidative-addition process (see below).

Reactions of $Ru(CO)_2(PPh_3)_3$ (1) with Disulfides. The formation of the bis(mercapto) series *cct*-$Ru(SH)_2(CO)_2(PPh_3)_2$ from **2a** is readily accomplished by treatment with H_2S around room temperature (eq 2) and could involve protonation of the metal

$$\underset{\mathbf{2a}}{RuH(SH)(CO)_2(PPh_3)_2} + H_2S \rightarrow \underset{\mathbf{3a}}{Ru(SH)_2(CO)_2(PPh_3)_2} + H_2 \quad (2)$$

hydride to liberate H_2 and generate a vacant site for attack by SH^-;[3,11] also possible is coordination of H_2S at a site vacated by a labile phosphine ligand, followed by elimination of H_2 and recoordination of the phosphine. There is much less tendency for the hydrido thiolato complexes (e.g. **2b,g**) to form the bis(thiolato) species (**3b,g**) via the corresponding reaction with RSH. The **3e–g** complexes containing arenethiolates, however, are cleanly formed by oxidative addition of the disulfide to **1** (eq 3), and the isolated **3g** complex has been characterized crystallographically (see below).

$$Ru(CO)_2(PPh_3)_3 + RSSR \rightarrow Ru(SR)_2(CO)_2(PPh_3)_2 + PPh_3 \quad (3)$$

The rate of reaction 3 using di-*p*-tolyl disulfide in C_6D_6, as monitored by $^{31}P\{^1H\}$ NMR spectroscopy, was unchanged in the presence of a thiyl-radical trap, suggesting a nonradical mechanism. A plausible process involves oxidative addition of the disulfide to the intermediate formed by loss of PPh_3:

$$\mathbf{1} \underset{k_{-1}, L}{\overset{k_1, -L}{\rightleftharpoons}} Ru(CO)_2L_2 \xrightarrow[RSSR]{k_2} Ru(SR)_2(CO)_2L_2 \ (L = PPh_3) \quad (4)$$

(21) Boniface, S. M.; Clark, G. R.; Collins, T. J.; Roper, W. R. *J. Organomet. Chem.* **1981**, *206*, 109.
(22) Pidcock, A.; Richards, R. E.; Venanzi, L. M. *J. Chem. Soc. A* **1966**, 1707.
(23) Sanchez-Delgado, R. A.; Thewalt, U.; Valencia, N.; Andriollo, A.; Macquez-Silva, R. L.; Puga, J.; Schollhorn, H.; Klein, H. P.; Fontal, B. *Inorg. Chem.* **1986**, *25*, 1097.
(24) Skapski, A. C.; Troughton, P. G. H. *J. Chem. Soc., Chem. Commun.* **1968**, 1230.
(25) Ball, R. G.; Trotter, J. *Inorg. Chem.* **1981**, *20*, 261.
(26) Hsieh, M.; Zingaro, R.; Krishnan, V. *Int. J. Sulfur Chem. A* **1971**, *1*, 197.
(27) Senoff, C. V. *Can. J. Chem.* **1970**, *48*, 2444.
(28) Singer, H.; Wilkinson, G. *J. Chem. Soc. A* **1968**, 2516.
(29) Farrar, D. H.; Grundy, K. R.; Payne, N. C.; Roper, W. R.; Walker, A. *J. Am. Chem. Soc.* **1979**, *101*, 6577.
(30) Keskinen, A. E.; Senoff, C. V. *J. Organomet. Chem.* **1972**, *37*, 201.
(31) Konno, T.; Kirchhoff, J. R.; Heineman, W. R.; Deutsch, E. *Inorg. Chem.* **1989**, *28*, 1174. Perkins, P. G.; Schultz, F. A. *Inorg. Chem.* **1983**, *22*, 1133.

Table IV. Final Atomic Coordinates (Fractional) and B(eq) Values

atom	x	y	z	B(eq), Å^2	atom	x	y	z	B(eq), Å^2
			(a) Ru(H)($SC_6H_4pCH_3$)$(CO)_2(PPh_3)_2$ (**2g**)						
Ru	0.39625 (2)	0.23433 (1)	0.36310 (2)	2.663 (7)	C(21)	0.5932 (2)	0.3756 (2)	0.2689 (2)	3.2 (1)
S	0.30451 (6)	0.28651 (5)	0.15245 (6)	4.10 (3)	C(22)	0.5912 (2)	0.4398 (2)	0.3638 (3)	4.1 (1)
P(1)	0.21506 (5)	0.22674 (4)	0.40562 (5)	2.80 (2)	C(23)	0.6022 (3)	0.5293 (2)	0.3375 (3)	5.3 (1)
P(2)	0.57093 (5)	0.25962 (4)	0.30634 (6)	2.89 (2)	C(24)	0.6153 (3)	0.5558 (2)	0.2174 (4)	5.8 (2)
O(1)	0.4931 (2)	0.2198 (2)	0.6397 (2)	6.4 (1)	C(25)	0.6170 (3)	0.4934 (2)	0.1246 (3)	5.5 (2)
O(2)	0.4235 (2)	0.0331 (2)	0.3080 (3)	7.2 (1)	C(26)	0.6069 (2)	0.4032 (2)	0.1495 (3)	4.2 (1)
C(1)	0.4578 (2)	0.2206 (2)	0.5347 (3)	4.0 (1)	C(27)	0.6091 (2)	0.1954 (2)	0.1718 (2)	3.5 (1)
C(2)	0.4098 (2)	0.1080 (2)	0.3212 (3)	4.1 (1)	C(28)	0.7179 (2)	0.1726 (2)	0.1651 (3)	4.5 (1)
C(3)	0.1218 (2)	0.3258 (2)	0.3689 (2)	3.3 (1)	C(29)	0.7471 (3)	0.1263 (2)	0.0624 (3)	5.3 (2)
C(4)	0.1576 (2)	0.4095 (2)	0.4061 (3)	4.6 (1)	C(30)	0.6689 (3)	0.1019 (3)	−0.0343 (3)	6.1 (2)
C(5)	0.0893 (3)	0.4860 (2)	0.3786 (3)	5.8 (2)	C(31)	0.5628 (3)	0.1239 (4)	−0.0291 (4)	9.3 (3)
C(6)	−0.0150 (3)	0.4796 (2)	0.3142 (3)	5.7 (2)	C(32)	0.5318 (3)	0.1698 (3)	0.0737 (4)	7.6 (2)
C(7)	−0.0512 (3)	0.3979 (2)	0.2761 (3)	5.2 (2)	C(33)	0.6875 (2)	0.2290 (2)	0.4309 (2)	3.1 (1)
C(8)	0.0166 (2)	0.3206 (2)	0.3025 (3)	4.3 (1)	C(34)	0.7742 (2)	0.2838 (2)	0.4650 (3)	4.1 (1)
C(9)	0.2141 (2)	0.2017 (2)	0.5736 (2)	3.4 (1)	C(35)	0.8616 (2)	0.2563 (2)	0.5575 (3)	5.0 (1)
C(10)	0.1798 (3)	0.2634 (2)	0.6568 (3)	5.2 (1)	C(36)	0.8636 (2)	0.1755 (2)	0.6177 (3)	4.9 (1)
C(11)	0.1915 (4)	0.2409 (3)	0.7859 (3)	7.5 (2)	C(37)	0.7784 (3)	0.1196 (2)	0.5830 (3)	4.8 (1)
C(12)	0.2354 (4)	0.1593 (3)	0.8294 (3)	7.1 (2)	C(38)	0.6909 (2)	0.1465 (2)	0.4907 (3)	4.1 (1)
C(13)	0.2689 (3)	0.0976 (3)	0.7477 (3)	5.8 (2)	C(39)	0.2654 (2)	0.4023 (2)	0.1460 (2)	3.6 (1)
C(14)	0.2595 (2)	0.1183 (2)	0.6206 (3)	4.5 (1)	C(40)	0.3239 (2)	0.4682 (2)	0.2124 (3)	4.6 (1)
C(15)	0.1332 (2)	0.1371 (2)	0.3287 (2)	2.97 (9)	C(41)	0.2911 (3)	0.5577 (2)	0.1958 (3)	5.3 (2)
C(16)	0.0491 (2)	0.1047 (2)	0.3843 (2)	3.6 (1)	C(42)	0.1987 (3)	0.5857 (2)	0.1115 (3)	5.4 (2)
C(17)	−0.0176 (2)	0.0407 (2)	0.3233 (3)	4.2 (1)	C(43)	0.1404 (3)	0.5200 (2)	0.0443 (3)	5.4 (2)
C(18)	0.0003 (2)	0.0078 (2)	0.2084 (3)	4.4 (1)	C(44)	0.1715 (2)	0.4300 (2)	0.0611 (3)	4.5 (1)
C(19)	0.0836 (2)	0.0391 (2)	0.1526 (3)	4.5 (1)	C(45)	0.1629 (4)	0.6837 (3)	0.0915 (4)	8.2 (2)
C(20)	0.1499 (2)	0.1038 (2)	0.2119 (2)	3.7 (1)	H(1)	0.390 (2)	0.336 (2)	0.405 (3)	5.4 (7)
			(b) Ru($SC_6H_4pCH_3$)$_2(CO)_2(PPh_3)_2$·THF (**3g**·THF)						
Ru	0.13050 (5)	0.21874 (4)	0.32473 (7)	2.66 (3)	C(25)	−0.1890 (7)	0.2895 (5)	−0.104 (1)	6.4 (6)
S(1)	0.1587 (2)	0.2929 (1)	0.1517 (2)	3.6 (1)	C(26)	−0.1681 (7)	0.2761 (4)	0.0285 (9)	4.9 (5)
S(2)	0.1947 (2)	0.1238 (1)	0.1380 (2)	3.7 (1)	C(27)	−0.0793 (5)	0.1302 (4)	0.2372 (7)	3.0 (4)
P(1)	0.3056 (2)	0.2177 (1)	0.4135 (2)	3.0 (1)	C(28)	−0.0908 (5)	0.1079 (4)	0.3650 (7)	3.1 (4)
P(2)	−0.0436 (1)	0.2150 (1)	0.2351 (2)	3.0 (1)	C(29)	−0.1096 (6)	0.0423 (4)	0.3712 (8)	3.8 (4)
O(1)	0.1126 (4)	0.1136 (3)	0.5150 (5)	4.7 (3)	C(30)	−0.1175 (6)	−0.0024 (4)	0.2516 (9)	4.3 (5)
O(2)	0.0592 (5)	0.3329 (3)	0.5611 (6)	5.8 (4)	C(31)	−0.1109 (6)	0.0202 (4)	0.1263 (8)	3.9 (4)
O(3)	0.468 (2)	0.4670 (8)	0.171 (1)	17 (1)	C(32)	−0.0910 (6)	0.0858 (4)	0.1178 (7)	3.7 (4)
C(1)	0.1182 (5)	0.1515 (4)	0.4409 (7)	2.8 (4)	C(33)	−0.1476 (6)	0.2759 (4)	0.3352 (7)	3.4 (4)
C(2)	0.0858 (6)	0.2920 (4)	0.4664 (8)	3.7 (4)	C(34)	−0.1390 (6)	0.3446 (4)	0.3693 (9)	4.7 (5)
C(3)	0.4197 (6)	0.1805 (4)	0.3016 (7)	3.1 (4)	C(35)	−0.2148 (7)	0.3936 (4)	0.447 (1)	6.3 (6)
C(4)	0.5130 (6)	0.1487 (4)	0.3539 (8)	4.0 (4)	C(36)	−0.3008 (7)	0.3731 (5)	0.489 (1)	6.5 (6)
C(5)	0.5985 (6)	0.1260 (4)	0.269 (1)	4.4 (5)	C(37)	−0.3127 (7)	0.3065 (5)	0.452 (1)	6.4 (6)
C(6)	0.5928 (7)	0.1344 (5)	0.132 (1)	5.3 (5)	C(38)	−0.2367 (6)	0.2580 (4)	0.3773 (9)	4.6 (5)
C(7)	0.4999 (7)	0.1665 (5)	0.0802 (8)	5.7 (5)	C(39)	0.0664 (5)	0.3736 (4)	0.1657 (8)	3.4 (4)
C(8)	0.4141 (6)	0.1897 (4)	0.1632 (8)	4.0 (4)	C(40)	0.0598 (6)	0.4250 (4)	0.2810 (8)	4.2 (5)
C(9)	0.3199 (5)	0.1696 (4)	0.5599 (7)	3.3 (4)	C(41)	−0.0121 (7)	0.4859 (4)	0.2860 (9)	4.7 (5)
C(10)	0.2799 (6)	0.2019 (5)	0.6875 (8)	4.5 (5)	C(42)	−0.0824 (7)	0.4983 (4)	0.180 (1)	4.8 (5)
C(11)	0.2801 (7)	0.1658 (6)	0.7988 (8)	5.3 (6)	C(43)	−0.0731 (7)	0.4486 (5)	0.0676 (9)	5.2 (5)
C(12)	0.3212 (7)	0.0952 (6)	0.781 (1)	5.6 (6)	C(44)	−0.0002 (7)	0.3862 (4)	0.0576 (8)	4.4 (5)
C(13)	0.3582 (7)	0.0613 (5)	0.656 (1)	5.5 (6)	C(45)	−0.1646 (8)	0.5640 (5)	0.187 (1)	7.6 (7)
C(14)	0.3578 (6)	0.0981 (4)	0.5434 (8)	4.2 (5)	C(46)	0.2398 (5)	0.0419 (4)	0.1963 (7)	3.1 (4)
C(15)	0.3422 (5)	0.3006 (4)	0.4846 (8)	3.5 (4)	C(47)	0.1718 (6)	0.0026 (4)	0.2349 (8)	3.8 (4)
C(16)	0.3114 (6)	0.3580 (5)	0.4167 (9)	4.9 (5)	C(48)	0.2081 (7)	−0.0649 (4)	0.2640 (7)	4.5 (5)
C(17)	0.3456 (8)	0.4199 (4)	0.462 (1)	6.1 (6)	C(49)	0.3116 (8)	−0.0948 (4)	0.2585 (9)	4.9 (5)
C(18)	0.4094 (7)	0.4233 (5)	0.576 (1)	6.0 (6)	C(50)	0.3789 (7)	−0.0552 (5)	0.224 (1)	5.9 (5)
C(19)	0.4409 (7)	0.3663 (5)	0.641 (1)	5.3 (5)	C(51)	0.3448 (6)	0.0120 (4)	0.1916 (8)	4.5 (5)
C(20)	0.4077 (6)	0.3058 (4)	0.5967 (8)	4.3 (5)	C(52)	0.3501 (9)	−0.1673 (5)	0.289 (1)	8.1 (7)
C(21)	−0.0744 (6)	0.2335 (4)	0.0578 (7)	3.5 (4)	C(53)	0.551 (2)	0.409 (2)	0.149 (3)	21 (2)
C(22)	−0.0051 (6)	0.2043 (4)	−0.0495 (8)	4.2 (5)	C(54)	0.523 (2)	0.357 (1)	0.069 (4)	25 (3)
C(23)	−0.0286 (8)	0.2187 (5)	−0.1814 (9)	5.7 (6)	C(55)	0.418 (2)	0.369 (1)	0.050 (2)	16 (2)
C(24)	−0.1201 (9)	0.2626 (6)	−0.210 (1)	6.6 (7)	C(56)	0.389 (2)	0.442 (2)	0.084 (3)	18 (2)
			(c) $[(PPh_3)(CO)_2Ru(SEt)_3Na(THF)]_2$ (**4**)						
Ru(1)	0.56768 (4)	0.18197 (3)	0.28424 (3)	3.26 (2)	C(6)	0.4279 (4)	0.5225 (4)	0.1305 (4)	4.0 (2)
S(1)	0.7506 (1)	0.0165 (1)	0.3369 (1)	6.05 (8)	C(7)	0.2778 (4)	0.3828 (4)	0.2776 (4)	3.6 (2)
S(2)	0.4531 (1)	0.0666 (1)	0.1457 (1)	4.04 (6)	C(8)	0.2392 (4)	0.4810 (4)	0.3404 (4)	4.2 (3)
S(3)	0.6480 (1)	0.1922 (1)	0.1263 (1)	4.12 (6)	C(9)	0.1514 (5)	0.4991 (5)	0.3966 (5)	5.8 (3)
P(1)	0.3992 (1)	0.34358 (8)	0.2063 (1)	3.15 (6)	C(10)	0.1005 (5)	0.4206 (6)	0.3879 (5)	6.4 (4)
Na(1)	0.6960 (2)	−0.0365 (2)	0.0905 (2)	5.0 (1)	C(11)	0.1359 (5)	0.3232 (5)	0.3245 (6)	6.3 (4)
O(1)	0.7373 (4)	0.2883 (3)	0.4683 (3)	7.3 (2)	C(12)	0.2237 (5)	0.3051 (4)	0.2698 (5)	5.0 (3)
O(2)	0.4763 (4)	0.1566 (3)	0.4777 (3)	7.2 (3)	C(13)	0.3039 (4)	0.3465 (3)	0.0488 (4)	3.4 (2)
O(3)	0.9066 (4)	−0.1109 (4)	0.0945 (4)	8.9 (3)	C(14)	0.1887 (4)	0.4310 (4)	0.0119 (4)	4.5 (3)
C(1)	0.4439 (4)	0.4662 (3)	0.2257 (4)	3.2 (2)	C(15)	0.1163 (5)	0.4402 (4)	−0.1058 (5)	5.5 (3)
C(2)	0.4975 (4)	0.5018 (4)	0.3398 (4)	3.9 (2)	C(16)	0.1583 (5)	0.3618 (5)	−0.1884 (4)	5.4 (3)
C(3)	0.5348 (5)	0.5925 (4)	0.3598 (4)	4.9 (3)	C(17)	0.2704 (5)	0.2781 (4)	−0.1549 (4)	4.6 (3)
C(4)	0.5178 (5)	0.6478 (4)	0.2649 (5)	5.4 (3)	C(18)	0.3441 (4)	0.2704 (3)	−0.0366 (4)	3.7 (2)
C(5)	0.4661 (5)	0.6135 (4)	0.1512 (5)	5.5 (3)	C(19)	0.7885 (7)	−0.0265 (7)	0.4795 (7)	10.9 (6)

Table IV (Continued)

atom	x	y	z	B(eq), Å²	atom	x	y	z	B(eq), Å²
C(20)	0.9046 (8)	−0.1152 (8)	0.5181 (8)	12.9 (7)	C(26)	0.5076 (5)	0.1663 (4)	0.4019 (4)	4.6 (3)
C(21)	0.4517 (6)	−0.0382 (4)	0.2263 (5)	6.3 (4)	C(27)	0.9580 (8)	−0.1873 (9)	0.0214 (8)	11.4 (7)
C(22)	0.3365 (7)	−0.0278 (7)	0.2348 (8)	11.3 (6)	C(28)	1.087 (1)	−0.242 (1)	0.090 (1)	18 (1)
C(23)	0.7955 (5)	0.2173 (5)	0.1933 (5)	6.0 (3)	C(29)	1.106 (1)	−0.203 (1)	0.205 (1)	15 (1)
C(24)	0.7799 (6)	0.3372 (6)	0.2072 (7)	8.6 (5)	C(30)	1.005 (1)	−0.101 (1)	0.194 (1)	17 (1)
C(25)	0.6699 (5)	0.2530 (4)	0.3947 (4)	4.6 (3)					

Table V. Selected Bond Lengths (Å) with Estimated Deviations in Parentheses[a]

(a) *cct*-$RuH(SC_6H_4pMe)(CO)_2(PPh_3)_2$ (**2g**)			
Ru–H(1)	1.58 (3)	P(1)–C(9)	1.835 (3)
Ru–C(1)	1.875 (3)	P(1)–C(15)	1.836 (2)
Ru–C(2)	1.945 (3)	P(2)–C(21)	1.825 (3)
Ru–P(1)	2.361 (1)	P(2)–C(33)	1.834 (3)
Ru–P(2)	2.381 (1)	P(2)–C(27)	1.837 (3)
Ru–S	2.458 (1)	O(1)–C(1)	1.136 (3)
S–C(39)	1.769 (3)	O(2)–C(2)	1.135 (3)
P(1)–C(3)	1.828 (3)		
(b) *cct*-$Ru(SC_6H_4pMe)_2(CO)_2(PPh_3)_2$ (**3g**)			
Ru–C(2)	1.863 (8)	P(1)–C(9)	1.814 (8)
Ru–C(1)	1.900 (8)	P(1)–C(15)	1.838 (8)
Ru–P(1)	2.444 (2)	P(1)–C(3)	1.841 (7)
Ru–P(2)	2.449 (2)	P(2)–C(33)	1.826 (7)
Ru–S(2)	2.450 (2)	P(2)–C(27)	1.833 (7)
Ru–S(1)	2.470 (2)	P(2)–C(21)	1.841 (7)
S(1)–C(39)	1.788 (7)	O(1)–C(1)	1.129 (7)
S(2)–C(46)	1.778 (8)	O(2)–C(2)	1.148 (8)
(c) $[(PPh_3)(CO)_2Ru(SEt)_3Na(THF)]_2$ (**4**)			
Ru(1)–S(1)	2.434 (2)	S(2)–C(21)	1.819 (5)
Ru(1)–S(2)	2.474 (1)	S(3)–Na(1)	2.821 (2)
Ru(1)–S(3)	2.467 (1)	S(3)–C(23)	1.825 (5)
Ru(1)–P(1)	2.375 (1)	P(1)–C(1)	1.839 (4)
Ru(1)–C(25)	1.865 (5)	P(1)–C(7)	1.834 (4)
Ru(1)–C(26)	1.877 (5)	P(1)–C(13)	1.840 (4)
S(1)–Na(1)	2.824 (2)	Na(1)–O(3)	2.365 (5)
S(1)–C(19)	1.746 (7)	O(1)–C(25)	1.144 (5)
S(2)–Na(1)	3.019 (2)	O(2)–C(26)	1.146 (5)
S(2)–Na(1)*	2.839 (2)		

[a] Asterisk denotes symmetry operation $1 - x, -y, -z$.

Table VI. Selected Bond Angles (deg) with Estimated Deviations in Parentheses[a]

(a) *cct*-$RuH(SC_6H_4pMe)(CO)_2(PPh_3)_2$ (**2g**)			
H(1)–Ru–C(1)	81 (1)	C(39)–S–Ru	113.6 (1)
H(1)–Ru–C(2)	176 (1)	C(3)–P(1)–C(9)	105.4 (1)
H(1)–Ru–P(1)	87 (1)	C(3)–P(1)–C(15)	102.3 (1)
H(1)–Ru–P(2)	88 (1)	C(3)–P(1)–Ru	117.53 (9)
H(1)–Ru–S	87 (1)	C(9)–P(1)–C(15)	101.1 (1)
C(1)–Ru–C(2)	96.0 (1)	C(9)–P(1)–Ru	111.35 (8)
C(1)–Ru–P(1)	92.80 (9)	C(15)–P(1)–Ru	117.30 (8)
C(1)–Ru–P(2)	91.59 (9)	C(21)–P(2)–C(33)	103.3 (1)
C(1)–Ru–S	167.2 (1)	C(21)–P(2)–C(27)	104.4 (1)
C(2)–Ru–P(1)	93.79 (8)	C(21)–P(2)–Ru	115.49 (8)
C(2)–Ru–P(2)	91.64 (8)	C(33)–P(2)–C(27)	101.2 (1)
C(2)–Ru–S	96.7 (1)	C(33)–P(2)–Ru	113.98 (8)
P(1)–Ru–P(2)	172.63 (3)	C(27)–P(2)–Ru	116.71 (9)
P(1)–Ru–S	84.04 (4)	O(1)–C(1)–Ru	174.3 (3)
P(2)–Ru–S	90.39 (4)	O(2)–C(2)–Ru	173.4 (3)
(b) *cct*-$Ru(SC_6H_4pMe)_2(CO)_2(PPh_3)_2$ (**3g**)			
C(2)–Ru–C(1)	91.6 (3)	C(46)–S(2)–Ru	113.6 (2)
C(2)–Ru–P(1)	86.8 (2)	C(9)–P(1)–C(15)	103.2 (4)
C(2)–Ru–P(2)	94.8 (2)	C(9)–P(1)–C(3)	106.3 (3)
C(2)–Ru–S(2)	178.1 (2)	C(9)–P(1)–Ru	107.0 (2)
C(2)–Ru–S(1)	95.9 (2)	C(15)–P(1)–C(3)	98.4 (3)
C(1)–Ru–P(1)	88.3 (2)	C(15)–P(1)–Ru	119.3 (3)
C(1)–Ru–P(2)	90.1 (2)	C(3)–P(1)–Ru	120.7 (2)
C(1)–Ru–S(2)	89.4 (2)	C(33)–P(2)–C(27)	103.1 (3)
C(1)–Ru–S(1)	172.3 (2)	C(33)–P(2)–C(21)	101.9 (3)
P(1)–Ru–P(2)	177.8 (1)	C(33)–P(2)–Ru	114.3 (3)
P(1)–Ru–S(2)	91.62 (8)	C(27)–P(2)–C(21)	103.5 (3)
P(1)–Ru–S(1)	90.64 (8)	C(27)–P(2)–Ru	113.0 (2)
P(2)–Ru–S(2)	86.87 (8)	C(21)–P(2)–Ru	119.1 (2)
P(2)–Ru–S(1)	90.74 (8)	O(1)–C(1)–Ru	176.7 (6)
S(2)–Ru–S(1)	83.05 (7)	O(2)–C(2)–Ru	174.2 (7)
C(39)–S(1)–Ru	113.0 (2)		
(c) $[(PPh_3)(CO)_2Ru(SEt)_3Na(THF)]_2$ (**4**)			
S(1)–Ru(1)–S(2)	88.46 (5)	Ru(1)–S(3)–Na(1)	85.91 (6)
S(1)–Ru(1)–S(3)	84.60 (5)	Ru(1)–S(3)–C(23)	109.4 (2)
S(1)–Ru(1)–P(1)	170.79 (5)	Na(1)–S(3)–C(23)	109.3 (2)
S(1)–Ru(1)–C(25)	84.6 (1)	Ru(1)–P(1)–C(1)	114.2 (1)
S(1)–Ru(1)–C(26)	93.4 (1)	Ru(1)–P(1)–C(7)	112.3 (1)
S(2)–Ru(1)–S(3)	88.47 (5)	Ru(1)–P(1)–C(13)	120.6 (1)
S(2)–Ru(1)–P(1)	90.33 (5)	C(1)–P(1)–C(7)	104.8 (2)
S(2)–Ru(1)–C(25)	173.0 (1)	C(1)–P(1)–C(13)	102.6 (2)
S(2)–Ru(1)–C(26)	89.2 (1)	C(7)–P(1)–C(13)	100.4 (2)
S(3)–Ru(1)–P(1)	86.25 (5)	S(1)–Na(1)–S(2)	71.64 (6)
S(3)–Ru(1)–C(25)	91.6 (2)	S(1)–Na(1)–S(2)*	157.14 (9)
S(3)–Ru(1)–C(26)	176.9 (1)	S(1)–Na(1)–S(3)	71.50 (6)
P(1)–Ru(1)–C(25)	96.6 (1)	S(1)–Na(1)–O(3)	95.3 (1)
P(1)–Ru(1)–C(26)	95.7 (1)	S(2)–Na(1)–S(2)*	85.79 (7)
C(25)–Ru(1)–C(26)	90.5 (2)	S(2)–Na(1)–S(3)	72.25 (6)
Ru(1)–S(1)–Na(1)	86.45 (6)	S(2)–Na(1)–O(3)	166.9 (1)
Ru(1)–S(1)–C(19)	114.0 (3)	S(2)*–Na(1)–S(3)	105.59 (8)
Na(1)–S(1)–C(19)	147.9 (3)	S(2)*–Na(1)–O(3)	107.3 (1)
Ru(1)–S(2)–Na(1)	81.57 (5)	S(3)–Na(1)–O(3)	104.2 (1)
Ru(1)–S(2)–Na(1)*	145.88 (6)	Na(1)–O(3)–C(27)	129.1 (5)
Ru(1)–S(2)–C(21)	110.1 (2)	Na(1)–O(3)–C(30)	123.0 (5)
Na(1)–S(2)–Na(1)*	94.21 (7)	C(27)–O(3)–C(30)	106.2 (6)
Na(1)–S(2)–C(21)	103.7 (2)	Ru(1)–C(25)–O(1)	173.8 (4)
Na(1)*–S(2)–C(21)	103.8 (2)	Ru(1)–C(26)–O(2)	176.8 (5)

[a] Asterisk denotes symmetry operation $1 - x, -y, -z$.

Such a mechanism has been established for reactions of H_2 and CO with **1** in DMA to give $Ru(H)_2(CO)_2(PPh_3)_2$ and $Ru(CO)_3(PPh_3)_2$, respectively, and the rate-limiting k_1 step has been estimated at about 0.1 s^{-1} at 24 °C.[5] Attempts to establish the mechanism of reaction 3 in benzene by measuring rates in the presence of added PPh_3 were thwarted by accompanying formation of some of the hydrido thiolato species **2g** and $OPPh_3$; these likely result from a side reaction involving trace water:[32]

$$RSSR + PPh_3 + H_2O \rightarrow 2RSH + OPPh_3$$

Reaction 3 using di-*p*-tolyl disulfide has been studied in THF by UV/vis spectroscopy:[33] kinetic data at 26 °C reveal a first-order dependence on **1** (at 0.1–0.7 mM) and a rate that goes from first to zero order in disulfide with increasing concentration of the disulfide from 2.5 to 50 mM. The findings are qualitatively consistent with the mechanism outlined in eq 4, but there is an unusually high scatter in the observed rates and the limiting rate at high [RSSR] corresponds to a k_1 value of $\sim 7 \times 10^{-3}$ s^{-1}, about 1 order of magnitude less than that measured in DMA for the H_2 and CO reactions.

The reaction of **1** with EtSSEt in benzene is much slower than that with di-*p*-tolyl disulfide under comparable conditions and also gives some of the hydrido thiolato species **2c**, as well as the expected **3c** product; the rate difference, if the mechanism of eq 4 applies, implies contributions of k_2 terms in the observed rates (rate = $k_1k_2[1][RSSR]/(k_{-1}[PPh_3] + k_2[RSSR])$) and a smaller k_2 value in the EtSSEt system, consistent with oxidative addition of the weaker Lewis acid.

Since our initial communication on the two cct complexes **3a** and **3g**,[3] other reports have described some $Ru(SR)_2(CO)_2(PPh_3)_2$ species including other isomers.[34] Table II lists some spectroscopic

(32) Overman, L. E.; Matzinger, D.; O'Connor, E. M.; Overman, J. D. *J. Am. Chem. Soc.* **1974**, *96*, 6081.
(33) Jessop, P. G. Ph.D. Dissertation, University of British Columbia, Vancouver, BC, Canada, 1991.

data from the present work for the isolated and in situ *cct*-bis(thiolato) complexes, including some mixed examples formed from reaction of *cct*-$Ru(H)_2(CO)_2(PPh_3)_2$ with binary mixtures of thiols (eq 5 (n = 0–2)). The cct geometry of the **3** complexes is

$$Ru(H)_2(CO)_2(PPh_3)_2 + nRSH + (2-n)R'SH \rightarrow Ru(SR)_n(SR')_{2-n}(CO)_2(PPh_3)_2 + 2H_2 \quad (5)$$

established by (a) the $^{31}P\{^1H\}$ NMR singlet of the phosphines, shown to be trans by the ^1H NMR data for the PPh_3 phenyl protons[16b] (see above), (b) the triplet pattern for the mercapto protons of **3a**, **3ae**, and **3ag**, at about 1.1–1.2 ppm downfield of the corresponding doublet of triplets signal for **2a**, (c) the ^1H signal of the Me group in **3g** being at the same shift as in the hydrido thiolato analogue **2g**, (d) two strong ν(CO) bonds characteristic of *cis*-carbonyls, (e) the X-ray structures of **3a**[11] and **3g** (see below), and (f) a comparison with $RuCl_2(CO)_2(PR_3)_2$ complexes in which the cct isomer is always the most stable.[35]

The ^{31}P chemical shifts vary little with the nature of the thiolate group(s), but empirically the shift of the *cct*-$Ru(SR)(SR')(CO)_2(PPh_3)_2$ species in C_6D_6 is roughly predicted by the additivity rule:

$$\delta, \text{ppm} = 10.67 + X(R) + X(R')$$

where

R =	H	C_6F_5	Et	C_6H_4pMe	Ph
X =	5.4	3.79	0.27	0.10	0.00

Catala et al. have synthesized the *cct*-$Ru(SR)_2(CO)_2(PPh_3)_2$ complexes (R = Me, *t*-Bu, C_6F_4H, C_6F_5) by carbonylation of $Ru(SR)_3(PPh_3)_2$ in the presence of Zn in acetone;[34] the spread of the reported ^{31}P shifts (in $CDCl_3$, relative to $P(OMe)_3$) is similar to that found here. However, after conversion to shifts relative to 85% H_3PO_4 (using a reported 141 ppm shift for $P(OMe)_3$),[36] the reported shifts[34b] are ~10 ppm to lower field than our values (e.g. for the common SC_6F_5 complex, 29.4 vs 18.30 ppm); the differences seem larger than expected even allowing for the different solvent used.

The series of **3** complexes show an absorption maximum in the UV/vis spectrum in THF, which again likely results from a thiolate ligand-to-metal charge transfer: for **3a**, λ_{max} at 371 nm (ϵ = 2460 M^{-1} cm^{-1}); for **3g**, λ_{max} 430 (ϵ = 3040).

The X-ray structure of **3g** (Figure 3; Tables IV–VI) confirms the cct geometry. The slight deviations from octahedral geometry at the Ru center (C(1)–Ru–C(2) = 91.6°, S(1)–Ru–S(2) = 83.05°) result from the PPh_3 groups crowding the carbonyl in order to avoid the bulky thiolate ligands. The proximity of the S atoms in **3g** is probably caused by the bulky *p*-tolyl groups which point away from each other; the S atoms are not so close together (3.26 Å) as to indicate S–S attractive interactions, which have been reported for some cis-thiolate complexes when the (sp^3) sulfur lone pairs overlap.[37] Visual inspection of the structure of this complex shows that the thiolate ligands are oriented so as to allow almost no lone-pair overlap. The S–S interatomic distance is close to that in *ccc*-$Fe(SPh)_2(CO)_2(PPh_2(CH_2)_2PPh_2)$[20] and is considerably longer than that observed in $Os(\eta^2\text{-}S_2Me)(CO)_2(PPh_3)_2$ (2.022 Å).[38] The lengths of the Ru–S, Ru–C, and C–O bonds are similar to those in **2g** (see above); the Ru–P bond lengths (average 2.446 Å) are greater than those in **2g** (average 2.371 Å) because of steric reasons, and the correlation with ^{31}P chemical shifts has been noted above (Figure 2). Structures related to **3g** are those of *cct*-$Ru(OCOPh)_2(CO)_2(PPh_3)_2$[39] and *ccc*-$Os(SC_6F_5)_2(CO)_2(PEt_2Ph)_2$.[40]

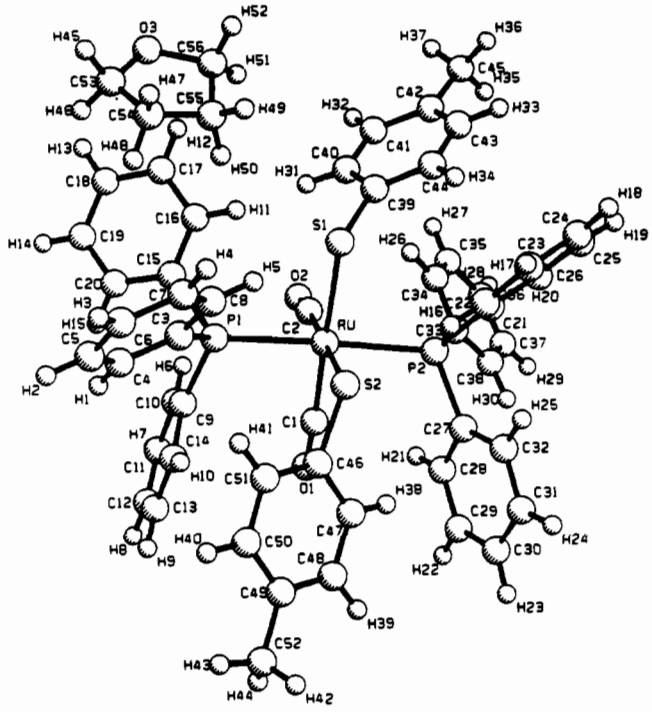

Figure 3. Structure of *cct*-$Ru(SC_6H_4pMe)_2(CO)_2(PPh_3)_2$·THF (**3g**·THF).

Reactions of $Ru(CO)_2(PPh_3)_3$ (1) with Thioethers and $Ru(CO)_3(PPh_3)_2$ with H_2S. Complex **1** in THF shows no reaction with Me_2S, Ph_2S, $PhSCH_2Ph$, or thiophene overnight at room temperature, but with the strained, cyclic thioether propylene sulfide, *cct*-$Ru(\eta^2\text{-}S_2)(CO)_2(PPh_3)_2$ is formed. Triphenylphosphine sulfide is also formed, and the stoichiometry of eq 6 seems likely,

$$1 + 3CH_2SCHCH_3 \rightarrow RuS_2(CO)_2(PPh_3)_2 + SPPh_3 + 3CH_2CHCH_3 \quad (6)$$

although the propene production was not confirmed experimentally. Triphenylphosphine itself does not abstract sulfur from propylene sulfide under the reaction conditions, implying that the Ru center is involved in this process. The ruthenium–disulfur product has been made previously from the reaction of **1** with elemental sulfur, but the only characterization reported was the ν(CO) values.[41]

The $Ru(CO)_3(PPh_3)_2$ complex is much less reactive than **1** toward H_2S (and thiols); with 1 atm of H_2S, only low conversions to **2a** and **3a** are realized under refluxing conditions in THF, the latter being formed from the former, as shown in eq 2. Related reactions of the tricarbonyl bis(phosphine) complex involve the formation of $Ru(pyS)_2(CO)_2(PPh_3)$ using pyridine-2-thiol[42] and formation of $RuX_2(CO)_2(PPh_3)_2$ species using HX reagents (X = Cl, Br, OCOR).[39,43] The favored mechanism[42] for these HX reactions is protonation, followed by replacement of CO by X to give, for example, $Ru(H)X(CO)_2(PPh_3)_2$, and then subsequent reaction with a second mole of HX to generate the product and H_2; the pathways contrast with those favored for $Ru(CO)_2(PPh_3)_3$ where initial dissociation of PPh_3 is evident (see above).

Metathesis Reactions of Chlororuthenium(II) Complexes with Thiolate Salts. Metathesis reactions of transition-metal chlorides with thiolate salts (or thiol plus base) provide a common synthetic

(34) (a) Catala, R. M.; Cruz-Garritz, D.; Terreros, P.; Torrens, H.; Hills, A.; Hughes, D. L.; Richards, R. L. *J. Organomet. Chem.* **1987**, *328*, C37. (b) Catala, R. M.; Cruz-Garritz, D.; Torrens, H.; Richards, R. L. *J. Organomet. Chem.* **1988**, *354*, 123. (c) Catala, R. M.; Cruz-Garritz, D.; Hills, A.; Hughes, D. L.; Richards, R. L.; Sosa, P.; Torrens, H. *J. Chem. Soc., Chem. Commun.* **1987**, 261.
(35) Krassowski, D. W.; Nelson, J. H.; Brower, K. R.; Hauenstein, D.; Jacobson, R. A. *Inorg. Chem.* **1988**, *27*, 4294.
(36) Crutchfield, M. M.; Dungan, C. H.; VanWazer, J. R. *Top. Phosphorus Chem.* **1967**, *5*, 1.
(37) Blower, P. J.; Dilworth, J. R. *Coord. Chem. Rev.* **1987**, *76*, 121.
(38) Clark, G. R.; Russell, D. R. *J. Organomet. Chem.* **1979**, *173*, 377.
(39) Rotem, M.; Stein, Z.; Shvo, Y. *J. Organomet. Chem.* **1990**, *387*, 95.
(40) Cruz-Garritz, D.; Sosa, P.; Torrens, H.; Hills, A.; Hughes, D. L.; Richards, R. L. *J. Chem. Soc., Dalton Trans.* **1989**, 419.
(41) Clark, G. R.; Russell, D. R.; Roper, W. R.; Walker, A. *J. Organomet. Chem.* **1977**, *136*, C1.
(42) (a) Collman, J. P.; Roper, W. R. *J. Am. Chem. Soc.* **1965**, *87*, 4008. (b) Robinson, S. D.; Uttley, M. F. *J. Chem. Soc., Dalton Trans.* **1973**, 1912.
(43) Collman, J. P.; Roper, W. R. *J. Am. Chem. Soc.* **1966**, *88*, 3504.

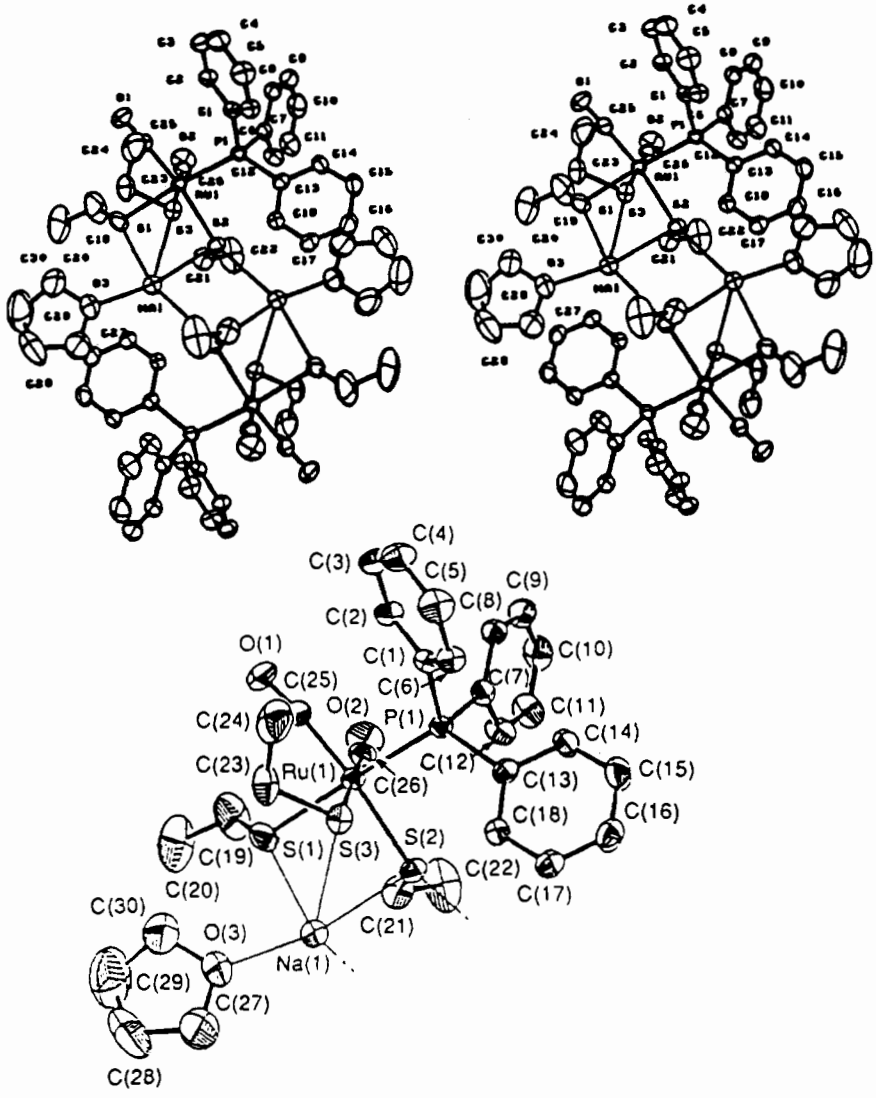

Figure 4. Stereoscopic view and atom-labeling diagram for the structure of $[(PPh_3)(CO)_2Ru(\mu_2\text{-}SEt)_2(\mu_3\text{-}SEt)Na(THF)]_2$ (**4**). H atoms are omitted for clarity.

route to thiolate complexes. The *cct*-$RuCl_2(CO)_2(PPh_3)_2$ precursor has been used to synthesize $Ru(pyS)_2(CO)_2(PPh_3)$ and $Ru(pyS)_2(CO)(PPh_3)$ containing chelated pyS (*o*-SC_5H_4N),[17] while the analogous *tcc*-dichloro precursor gives *tcc*-$Ru(SR)_2(CO)_2(PPh_3)_2$ complexes.[34b] The driving force for the reactions is the precipitation of an insoluble salt (e.g. NaCl, $PbCl_2$). Isomers of $Ru(SR)_2(CO)_2(PPh_3)_2$ have been made also by metathesis reactions of chloro(phosphine)ruthenium(II or III) species followed by carbonylation using 1 atm of CO.[34,44]

We successfully prepared the bis (*p*-thiocresolate) complex **3g** by metathesis of *cct*-$RuCl_2(CO)_2(PPh_3)_2$ with the sodium thiolate, the synthesis providing an alternative route to that shown in eq 3. The metathesis reaction with sodium ethanethiolate in acetone produces the bis(thiolate) **3c**, but its purification is plagued by formation of intractable oils. The corresponding reaction in THF generates *cct*-$RuCl(SEt)(CO)_2(PPh_3)_2$ (**5**) and **3c**, in varying ratios depending on the amount of thiolate and the reaction time used; $[(PPh_3)(CO)_2Ru(SEt)_3Na(THF)]_2$ (**4**) is obtained pure from reactions using ≥20 equiv of thiolate and reaction times ≥1 h (eq 7).

$$2Ru(SEt)_2(CO)_2(PPh_3)_2 + 2NaSEt \xrightarrow{THF} \mathbf{4} + 2PPh_3 \qquad (7)$$

Within **5**, the 1.25 ppm chemical shift difference between the *o*-H and the *m*-, *p*-H phenyl protons again indicates trans phosphines, whose $^{31}P\{^1H\}$ singlet at 14.54 ppm is between those of *cct*-$RuCl_2(CO)_2(PPh_3)_2$ (15.66 ppm) and *cct*-$Ru(SEt)_2(CO)_2(PPh_3)_2$ (**3c**) (11.18 ppm); the IR data again reveal cis carbonyls, and so the geometry of **5** is again cct. Worth noting is that the ^1H NMR shifts of the ethyl groups in **5**, which are very similar to those of **3c**, are some 0.6–0.7 ppm to lower fields than the ethyl group of *cct*-$RuH(SEt)(CO)_2(PPh_3)_2$ (**2c**), reflecting perhaps the electron-withdrawing character of Cl^- and SEt^- vs H^-.

The reaction of a $RuCl_3/PPh_3$ mixture with NaSEt and CO was attempted because of a report of a similar, attractive synthesis for *cct*-$Ru(SC_6F_5)_2(CO)_2(PMePh_2)_2$ directly from $RuCl_3$.[34b] However, a complex mixture containing *cct*-$RuX_2(CO)_2(PPh_3)_2$ (X_2 = Cl_2, Cl and SEt, $(SEt)_2$), a species with a $^{31}P\{^1H\}$ singlet at the same position as for **4** (presumably the MeOH analogue of **4**), and other unknowns was obtained.

Reaction of *cct*-$RuH(Cl)(CO)_2(PPh_3)_2$ with 1 equiv of $NaSC_6H_4pMe$ gave 55% conversion to the hydrido thiolate **2g**, while use of 3 equiv of the sodium thiolate gave 90% conversion to the bis(thiolate) complex **3g**. The preferred synthetic route to **2g** is the reaction of $Ru(CO)_2(PPh_3)_3$ with the thiol, however, because coformation of **3g** is avoided.

$[(PPh_3)(CO)_2Ru(\mu\text{-}SEt)_3Na(THF)]_2$ (4). The X-ray structure of **4** (Figure 4; Tables IV–VI) has an imposed crystallographic center of symmetry, and hence only half of the atoms are labeled. The two Ru atoms are connected by a network of six bridging thiolates and two sodium atoms; four thiolates (S(1), S(3), S(1)*, S(3)*) bridge one Ru and one Na, and two thiolates (S(2), S(2)*)

(44) Catala, R. M.; Cruz-Garritz, D.; Sosa, P.; Terreros, P.; Torrens, H.; Hills, A.; Hughes, D. L.; Richards, R. L. *J. Organomet. Chem.* **1989**, *359*, 219.

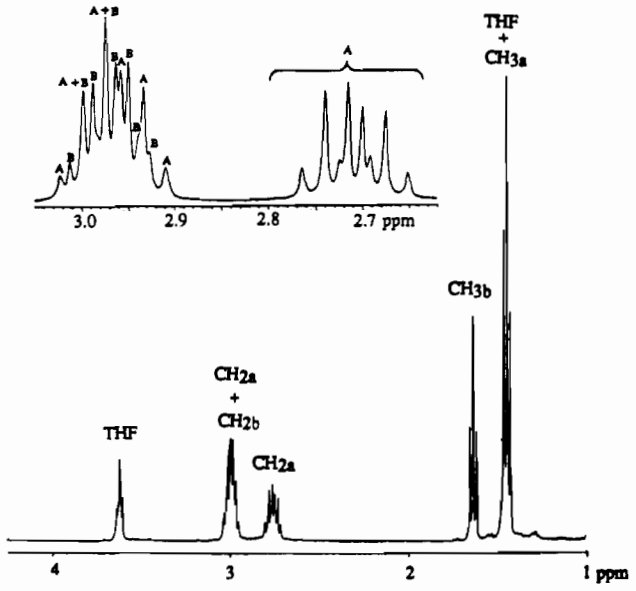

Figure 5. A region of the ^1H NMR spectrum (400 MHz) of $[(PPh_3)(CO)_2Ru(\mu\text{-}SEt)_3Na(THF)]_2$ (**4**) in C_6D_6 at 20 °C. In the expanded methylene region, the $CH_2(a)$ and $CH_2(b)$ protons are identified by the letters A and B, respectively, the peak positions matching within 0.005 ppm those of a spectrum simulated by the quoted δ and J values.

bridge one Ru and two Na atoms. Alternatively, each Na atom is bound to three thiolate ligands of one $Ru(SEt)_3(CO)_2(PPh_3)$ fragment, one thiolate of the other fragment, and a THF molecule. The Na has distorted square-pyramidal geometry, the available sixth site (trans to S(3)) being blocked by a phenyl group of PPh_3. The *cis*-S–Na–S angles are 71 or 72°, except those involving S(2)*, because the Na is shifted toward the sixth site, while the *cis*-S–Na–O angles are >90° because the THF also leans toward the sixth site; the Na–S bond lengths within the μ_2-thiolate moieties are comparable to that found in NaSMe (2.8 Å).[45]

There are three types of thiolates present: one (S(1)) doubly bridging trans to PPh_3, one (S(3)) doubly bridging trans to a CO, and one (S(2)) triply bridging trans to a CO. The geometry at Ru is essentially octahedral; the Ru–S bond lengths of the thiolate ligands trans to carbonyls (2.474, 2.467 Å) are essentially identical to those noted in structure **2g** and **3g**·THF described above. The Ru–S and the S–C bond lengths for the S(1) thiolate trans to PPh_3 (2.434 and 1.746 Å, respectively) are somewhat shorter than in the S(2) and S(3) thiolate ligands because of relative trans influences (PPh_3 < CO); the Ru–S bond length of a similar thiolate ligand in $Ru(pyS)_2(CO)_2(PPh_3)$ is comparable (2.42 Å).[17a] As expected, the S–C(sp^3) bond lengths in **4** are longer than the S–C(sp^2) bond lengths within the arenethiolate-containing structures **2g** and **3g**. The Ru–C and C–O bond lengths of **4** are close to those in the CO ligands trans to thiolates in **2g** and **3g**.

The triple bridging between a transition-metal and an alkali-metal ion, as observed in **4**, is unprecedented. The recently reported anionic species $[Na\{Ru(CO)_2(Se_4)_2\}_2]^{3-}$ contains Se atoms (of Se_4^{2-} ligands) bridging Ru and Na atoms,[46] while examples of alkanethiolates bridging three Ru atoms are known.[47] More generally there are few examples of transition-metal complexes containing alkali-metal cations "trapped" via bridging thiolate ligands: $(SC_6H_4pMe)_3Nb(\mu\text{-}SC_6H_4pMe)_3Na(THF)_3$,[48] $(C_5Me_5)_2Lu(\mu\text{-}S^tBu)_2Li(THF)_2$,[49] and $[Li(dme)]_4[U(edt)_4]$(dme = 1,2-dimethoxyethane; edt = 1,2-ethylenedithiolate).[50] There are many more examples of trapped alkali-metal cations in alkoxide chemistry, particularly in byproducts of metathesis reactions using alkoxide salts.[51]

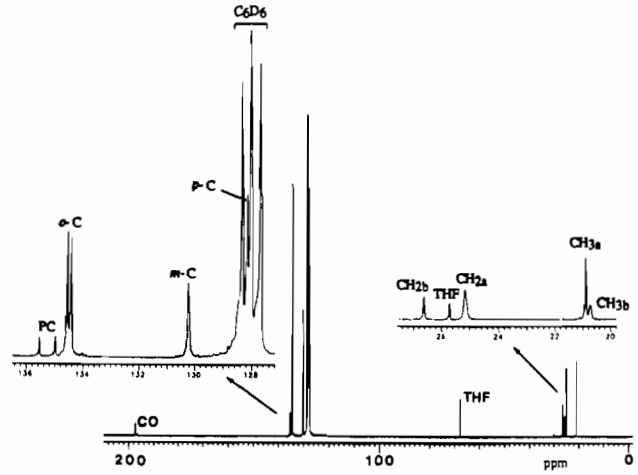

Figure 6. $^{13}C\{^1H\}$ NMR spectrum (75 MHz) of **4** in C_6D_6 at 20 °C. The resonances are also listed in the Experimental Section.

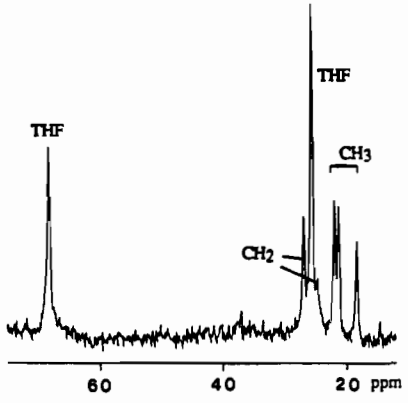

Figure 7. Solid-state ^{13}C (CP/MAS) NMR spectrum of **4**.

An anion containing a Ru moiety of the kind found in **4** is $RuI_3(CO)_2(PPh_3)^-$,[52] while others such as $RuX_3(CO)_3^-$ (X = halide)[53] and $RuCl_3(CO)(PPh_3)_2^-$[54] may be considered related.

The room-temperature solution structure of **4** appears to differ from that in the solid state. Lack of conductivity in THF solution shows that there is no significant dissociation into ions, but the ^1H NMR spectrum (in C_6D_6, Figure 5) shows that two of the thiolates at each Ru center are now magnetically equivalent. These are labeled *a* and are presumably the S(2) and S(3) thiolates trans to the carbonyls; *b* refers to the thiolate trans to PPh_3. The ^1H NMR spectrum, which shows the correct ligand ratios PPh_3:THF:Et(*a*):Et(*b*) = 1:1:2:1, was assigned with the help of a COSY experiment. The $CH_3(a)$ triplet coincides with that of the β-CH_2 protons of THF. The methylene region was resolved by irradiation of the CH_3 resonances; the $CH_2(a)$ protons appear as two doublets, while the $CH_2(b)$ protons are seen as a second-order AB pattern. The methylene region of the ^1H NMR spectrum is accurately simulated by the shifts and coupling constants given in the Experimental Section. The $^{31}P\{^1H\}$ singlet observed at room temperature broadens at lower temperature but is

(45) Weiss, E.; Joergens, U. *Chem. Ber.* **1972**, *105*, 481.
(46) Draganjac, M.; Dhingra, S.; Huang, S.-P.; Kanatzidis, M. G. *Inorg. Chem.* **1990**, *29*, 590.
(47) (a) Bruce, M. I.; Shawkataly, O. B.; Nicholson, B. K. *J. Organomet. Chem.* **1985**, *286*, 427. (b) Creswell, T. A.; Howard, J. A. K.; Kennedy, F. G.; Knox, S. A. R.; Wadepohl, H. *J. Chem. Soc., Dalton Trans.* **1981**, 2220.
(48) Koo, S.-M.; Bergero, R.; Salifoglou, A.; Coucouvanis, D. *Inorg. Chem.* **1990**, *29*, 4844.
(49) Schumann, H.; Albrecht, I.; Gallagher, M.; Hahn, E.; Muchmore, C.; Pickardt, J. *J. Organomet. Chem.* **1988**, *349*, 103.
(50) Tatsumi, K.; Matsubara, I.; Inoue, Y.; Nakamura, A.; Cramer, R. E.; Tagoshi, G. J.; Golen, J. A.; Gilje, J. W. *Inorg. Chem.* **1990**, *29*, 4928.
(51) (a) Bradley, D. C.; Mehrotra, R. C.; Gaur, D. P. *Metal Alkoxides*; Academic Press, Inc.: London, 1978; pp 299–334. (b) Caulton, K. G.; Hubert-Pfalsgraf, L. G. *Chem. Rev.* **1990**, *90*, 969.
(52) Jeffery, J.; Mawby, R. J. *J. Organomet. Chem.* **1972**, *40*, C42.
(53) (a) Cleare, M. J.; Griffith, W. P. *J. Chem. Soc. A* **1969**, 372. (b) Colton, R.; Farthing, R. H. *Aust. J. Chem.* **1971**, *24*, 903.
(54) Armit, P. W.; Sime, W. J.; Stephenson, T. A. *J. Chem. Soc., Dalton Trans.* **1976**, 2121.

uninformative [e.g., in toluene-d_8, $w_{1/2}$, Hz (T, °C): 8 (18), 29 (−58), 120 (−78)].

The solution $^{13}C\{^1H\}$ NMR spectrum of **4** (Figure 6) was assigned with the help of APT and HETCOR experiments. That only the two peaks $CH_2(a)$ and $CH_2(b)$ are seen confirms that the two Et(a) groups are equivalent, and the single more intense peak for the $CH_3(a)$ group supports this; the smaller $CH_3(b)$ signal appears inexplicably split in the $^{13}C\{^1H\}$ and APT spectra at 75 MHz but not in the $^{13}C\{^1H\}$ spectrum at 125 MHz. The ^{13}C assignments for the phenyl region are based on the premise that the J_{PC} value decreases for phenyl carbons in the order P-bound, o-, m-, and p-C.

The CP/MAS, solid-state ^{13}C NMR spectrum (Figure 7) contains two peaks for the THF ligands; the 25.6 ppm peak overlaps those of the methylenes of the Et groups, and only two instead of the expected three $-CH_2-CH_3$ resonances are seen. The three CH_3 signals associated with the three types of thiolate ligands are evident. An NQS ^{13}C experiment, in which strongly dipolar-coupled CH and CH_2 carbons are suppressed, and quaternary and rapidly moving groups such as CH_3 are detected,[55] gave a spectrum showing only the three higher field CH_3 peaks and that of the THF β-carbons; this experiment identifies the CH_3 resonances and also suggests that the THF β-carbons are relatively mobile, as suggested also by the size of their thermal ellipsoids in Figure 4; i.e., the THF ligand is "wagging".

There is the possibility that **4** becomes monomeric in solution via breaking of the Na–S(2)* and Na*–S(2) bonds, and this could account for the solution NMR data, if the resulting Na–S(2) and Na–S(3) bonds are equivalent. Unfortunately, **4** had insufficient solution stability for determination of its molecular weight by the Signer method[56] and insufficient solubility for a freezing-point depression experiment.

For the Et(a) groups attached to S(2) and S(3) to become equivalent within a dimeric unit, the following motions must occur rapidly on the NMR time scale: (a) inversion at S(1), (b) movement of Na* between S(2) and S(3) and Na between S(2)* and S(3)*, and (c) motion of THF between the sites trans to S(2) and S(3). Motion c would be impossible without dissociation of the THF ligand because of hindrance from the phenyl groups and would have to occur simultaneously with motion b. The ^1H and $^{13}C\{^1H\}$ shifts of the THF are not significantly different from those of free THF, and this is consistent with, but not proof of, THF dissociation. The noted inequivalence of the CH_2 (b) protons on C(19), however, implies noninversion at S(1), and kinetic data on the interconversion of anti and syn isomers of complexes such as $[Fe(CO)_3(\mu\text{-}SEt)]_2$ imply that such inversion would be slow at ambient conditions in solution.[57] The breakdown of **4** in solution to monomeric species seems likely.

Variable-temperature ^1H NMR spectra offer little insight into the problem: at ≥60 °C, **4** decomposes to unknown products, while at −78 °C the non-THF peaks of the complex are considerably broadened.

Acknowledgment. We thank the Natural Sciences and Engineering Research Council of Canada for financial support in the form of an operating grant (B.R.J.) and a postgraduate fellowship (P.G.J.), the Isaac Walton Killam Foundation for a postdoctoral fellowship (C.-L.L.), and Johnson Matthey Ltd. for the loan of Ru.

Registry No. **1**, 61647-76-5; **2a**, 107031-85-6; **2b**, 136823-89-7; **2c**, 107031-78-7; **2d**, 107031-79-8; **2e**, 107052-99-3; **2g**, 107031-82-3; **2h**, 107031-81-2; **2i**, 107031-80-1; **2f**, 136823-90-0; **3a**, 107031-86-7; **3ae**, 136823-93-3; **3ag**, 136823-92-2; **3c**, 136050-00-5; **3cg**, 136823-95-5; **3e**, 136890-88-5; **3ef**, 136823-94-4; **3eg**, 136823-96-6; **3f**, 118456-88-5; **3g**, 136823-91-1; **3g**·THF, 136823-98-8; **3h**, 136823-97-7; **4**, 136050-11-8; **5**, 136050-16-3; **6**, 32240-58-7; *cct*-$RuH_2(CO)_2(PPh_3)_2$, 21029-29-8; *cct*-$Ru(\eta^2\text{-}S_2)(CO)_2(PPh_3)_2$, 136890-87-4; $Ru(CO)_3(PPh_3)_2$, 14741-36-7; *cct*-$RuCl_2(CO)_2(PPh_3)_2$, 29079-66-1; $RuCl_2(PPh_3)_3$, 15529-49-4.

Supplementary Material Available: Tables S-I–S-V, listing elemental analyses of complexes **2a–e**, **2g–j**, **3a,g**, *cct*-$RuS_2(CO)_2(PPh_3)_2$ (**5**), and $[(PPh_3)(CO)_2Ru(SEt)_3Na(THF)]_2$, thermal parameters, bond distances and angles, and hydrogen atom parameters (27 pages); Tables S-VI–S-VIII, listing observed and calculated structure factors for **2g**, **3g**, and **4** (187 pages). Ordering information is given on any current masthead page.

(55) Opella, S. J.; Frey, M. H. *J. Am. Chem. Soc.* **1979**, *101*, 5854.
(56) Clark, E. P. *Ind. Eng. Chem., Anal. Ed.* **1941**, *13*, 820.
(57) (a) Ellgen, P. C.; Gerlach, J. N. *Inorg. Chem.* **1973**, *12*, 2526. (b) Natile, G.; Maresca, L.; Bor, G. *Inorg. Chim. Acta* **1977**, *23*, 37. (c) Lu, X. Q.; Zhu, C. Y.; Song, L. C.; Chen, Y. T. *Inorg. Chim. Acta* **1988**, *143*, 55.
(58) LaPlaca, S. J.; Ibers, J. A. *Inorg. Chem.* **1965**, *4*, 778. Hoffman, P. R.; Caulton, K. G. *J. Am. Chem. Soc.* **1975**, *97*, 4221.
(59) Dekleva, T. W.; Thorburn, I. S.; James, B. R. *Inorg. Chim. Acta* **1985**, *100*, 49. Hampton, C.; Dekleva, T. W.; James, B. R.; Cullen, W. R. *Inorg. Chim. Acta* **1988**, *145*, 165.
(60) Skapski, A. C.; Stephens, F. A. *J. Chem. Soc., Dalton Trans.* **1976**, 390.
(61) McConway, J. C.; Skapski, A. C.; Phillips, L.; Young, R. J.; Wilkinson, G. *J. Chem. Soc., Chem. Commun.* **1974**, 327.